

SBIR- 08.03-4520  
release date 1/06/90 ✓

rp

(NASA-CR-190868) A TEOM (TM)  
PARTICULATE MONITOR FOR COMET DUST,  
NEAR EARTH SPACE, AND PLANETARY  
ATMOSPHERES Final Report  
(Rupprecht and Patashnick Co.)  
73 p

093-10675

Unclass

03/90 0121103

**A TEOM® PARTICULATE MONITOR FOR  
COMET DUST, NEAR EARTH SPACE,  
AND PLANETARY ATMOSPHERES**

**FINAL REPORT  
NASA SBIR 84-1 PHASE II  
CONTRACT NAS7-962  
APRIL 1988**

submitted to

**NASA RESIDENT OFFICE  
JET PROPULSION LABORATORY  
CALIFORNIA INSTITUTE OF TECHNOLOGY  
4800 OAK GROVE DRIVE  
PASADENA, CA 91109**

submitted by

**RUPPRECHT AND PATASHNICK CO., INC.  
8 CORPORATE CIRCLE  
ALBANY, NY 12203**

518/452-0065

## TABLE OF CONTENTS

<u>Section</u>	<u>Page</u>
SUMMARY	1
1. Introduction to TEOM® Mass Monitor Sensors for Vacuum and Space Use	2
1.1 Brief History of Instrument Program	2
1.2 Description of Concept Instrument	3
1.3 Prototype Sensor Descriptions	5
1.4 Principle of Operation	5
1.5 Data Reduction Methods, Sample Data	8
2. Scope and Task Descriptions	16
2.1 Scope of Contract	16
2.2 Contract Tasks	17
3. Objectives	18
3.1 Performance, Sensor Specifications	19
3.2 Manufacturability	22
3.3 Quality Control	24
3.3.1 Influence of Quality Control Considerations on Design	24
3.3.2 Inspection Points	25
4. Results	26
4.1 Performance	26
4.1.1 Resolution	26
4.1.2 Stability	32
4.1.3 Dynamic Range	34
4.1.4 Temperature Coefficient	36
4.1.5 Environmental Factors	38
4.1.5.1 Vibration	38
4.1.5.2 Electrical Noise	39
4.2 Durability	40
4.3 Manufacturing and Quality Control	41
4.3.1 Materials	41
4.3.2 Processes	46
4.4 Drive Electronics	52
4.4.1 Schematic and Description	53
4.4.2 Parts List, Including Weights	56
4.4.3 Power Consumption	57
4.5 Flight-like Housing, Including Weight	58
5. Conclusions	58

6.	Brief Look at Work Remaining before Flight (Sensors Only)	59
6.1	Sticky Material Stability and Efficiency	59
6.2	Coordination of Instrument Design with Sensor Properties, Especially Temperature Control/compensation and Data Collection Scheme	59
6.3	Integration of Flight-ready Sensors into Flight Instrument	60
Appendix I	Vibration Test Results	
Appendix II	Specifications of All Sensors Cited	

## FIGURES

<u>No.</u>	<u>Title</u>	<u>Page</u>
1	Portable Version of Concept Instrument	4
2	Assembly Drawing	6
3	Eight Complete Mass Sensors	7
4	Sensor Operating Principle	7
5	Seven Particles Landing on a .01 cm <sup>2</sup> Sensor, 20 Second Averaging	12
6	Seven Particles Landing on a .01 cm <sup>2</sup> Sensor, 80 Second Averaging	13
7	Seven Particles Landing, 80 Second Averaged Difference Plot	14
8	Two Particles, Shown by 20 Sec Ave, 80 Sec Ave, 20 Sec Difference, and 80 Second Difference Plots	15
9	Averaging Time vs Resolution, .01 cm <sup>2</sup> Sensor	21
10	Resolution at 20 Second Averaging, .01 cm <sup>2</sup> Sensor	27
11	Resolution at 80 Second Averaging, .01 cm <sup>2</sup> Sensor	28
12	Resolution at 20 Second Averaging, .1 cm <sup>2</sup> Sensor	29
13	Resolution at 80 Second Averaging, .1 cm <sup>2</sup> Sensor	30
14	Resolution at 20 Second Averaging, 1 cm <sup>2</sup> Sensor	31
15	Resolution at 80 Second Averaging, 1 cm <sup>2</sup> Sensor	32
16	Drift of .1 cm <sup>2</sup> Sensor over Several Days	34
17	Temperature Coefficient of Frequency for Sensors with SiC Collection Stages	36
18	Temperature Coefficient of Frequency for Sensors with Be Collection Stages	37
19	Schematic of Analog Circuit	54

## SBIR RIGHTS NOTICE

This SBIR data is furnished with SBIR rights under NASA Contract No. NAS7-962. For a period of 2 years after acceptance of all items to be delivered under this contract the Government agrees to use this data for Government purposes only, and it shall not be disclosed outside the Government during such period without permission of the Contractor, except that, subject to the foregoing use and disclosure prohibitions, such data may be disclosed for use by support contractors. After the aforesaid 2-year period the Government has a royalty-free license to use, and to authorize others use on its behalf, this data for Government purposes, but is relieved of all disclosure prohibitions and assumes no liability for unauthorized use of this data by third parties. This Notice shall be affixed to any reproductions of this data, in whole or in part.

## SUMMARY

Scientific missions to comets, near earth space, and planetary atmospheres require particulate and mass accumulation instrumentation for both scientific and navigation purposes. The Rupprecht & Patashnick tapered element oscillating microbalance can accurately measure both mass flux and mass distribution of particulates over a wide range of particle sizes and loadings. Individual particles of milligram size down to a few picograms can be resolved and counted, and the accumulation of smaller particles or molecular deposition can be accurately measured using the sensors perfected and toughened under this contract. No other sensor has the dynamic range or sensitivity attained by these picogram direct mass measurement sensors.

The purpose of this contract was to develop and implement reliable and repeatable manufacturing methods; build and test prototype sensors; and outline a quality control program. A dust "thrower" was to be designed and built, and used to verify performance. Characterization and improvement of the optical motion detection system and drive feedback circuitry was to be undertaken, with emphasis on reliability, low noise, and low power consumption.

All the goals of the contract were met or exceeded. An automated glass puller was built and used to make repeatable tapered elements. Materials and assembly methods were standardized, and controllers and calibrated fixtures were developed and used in all phases of preparing, coating and assembling the sensors. Quality control and reliability resulted from the use of calibrated manufacturing equipment with measurable working parameters. Thermal and vibration testing of completed prototypes showed low temperature sensitivity and high vibration tolerance. An electrostatic dust thrower was used in vacuum to throw particles from  $2 \times 10^{-6}$  g to  $7 \times 10^{-12}$  g in size. Using long averaging times, particles as small as 0.7 to  $4 \times 10^{-11}$  g were weighed to resolutions in the  $5$  to  $9 \times 10^{-13}$  g range. The drive circuit and optics systems were developed beyond what was anticipated in the contract, and are now virtually flight prototypes.

There is already commercial interest in the developed capability of measuring picogram mass losses and gains. One area is contamination and outgassing research, both measuring picogram losses from samples and collecting products of outgassing.

# 1. Introduction to TEOM® Mass Monitor Sensors for Vacuum and Space Use

## 1.1 Brief History of Instrument Program

Rupprecht and Patashnick Co., Inc. (R&P) is the manufacturer and holder of patents for the tapered element oscillating microbalance (manufactured under the trade name TEOM®). R&P makes and sells laboratory and commercial inertial mass measuring instruments in a wide range of sensitivities. Early in the company's history ultra-high sensitivity laboratory microbalances were made for comet ice, comet dust, and outgassing studies with resolutions of  $1 \times 10^{-10}$  g. At a time when R&P's fully developed commercial product was a filter based microbalance with resolution of approximately  $1 \times 10^{-7}$  g, R&P was asked to develop a set of flight qualifiable TEOM® sensors which could capture and measure individual particles of comet dust. The request was for development of three sizes of sensors, with the most sensitive to have a resolution of at least  $1 \times 10^{-11}$  g. The two other sensors were specified nominally  $1 \times 10^{-10}$  g and  $1 \times 10^{-9}$  g. The highest resolution sensor would have a  $.01 \text{ cm}^2$  collection area, and the lower resolution sensors would have larger areas (.1 and  $1 \text{ cm}^2$ ) so that statistically significant numbers of large particles would be captured. (Large particles are much fewer in number than small ones in a comet environment.)

A program was begun to develop and improve the earth-bound ultra-high sensitivity microbalances into rugged and dependable flight instruments. The program was divided into two parts. JPL took responsibility for design of the flight instrument housing, counter, digital electronics, view limiters, shutters, power supplies, and thermal controls. R&P, through various JPL and NASA contracts, took responsibility for the design and prototyping of the sensors and analog sensing and driving electronics. R&P had built and perfected counters, digital electronics, and software for its commercial work; these were used for sensor development and provided a basis for JPL's design of the flight equipment. Various small contracts awarded to R&P proved the feasibility of making a "picobalance", a balance with short time mass resolution in the  $3$  to  $5 \times 10^{-12}$  g region. The most important part of this work was the selection of materials and the definition of the size and shape of the required tapered elements and collection stages. An independent effort by R&P and Corning Glass Works to develop a better glass for commercial balances provided a key material as well.

In 1985 JPL submitted a proposal to NASA for the Microbalance Ice and Dust Accumulation Sensor (MIDAS) experiment to fly on the Comet Rendezvous and Asteroid Flyby (CRAF) mission,

utilizing 8 TEOM® systems. In 1986, R&P was awarded an SBIR phase two award (this contract) to further develop sensors such as the ones needed for MIDAS. In addition to the comet science group proposing MIDAS for CRAF, there are at least two space station working groups interested in picogram sensitivity TEOM® instruments for contamination measurements.

## 1.2 Description of Concept Instrument

Because of the broadening interest in these ultra high sensitivity sensors and the present uncertainty about the number and type of sensors desired for the CRAF mission, a single sensor "instrument" will be described here and will be the "instrument" referred to throughout this report. A full description of the MIDAS configuration can be found in the MIDAS/CRAF proposal of Nov 1985 and Robert Wilson's update presented in Houston in Nov 1987. The definition of an instrument is a bit arbitrary, in that one can make various assumptions about available power and the form of output required. Power will be assumed to be available at standard voltages, (+/-15, +5) well regulated. Output will be assumed in the form of digital data supplied to a computer bus. A "number of cycles" count and a "duration" count comprise one data set, and these can be generated at intervals from .1 sec to 3 sec using R&P's standard, IBM PC compatible counter board. The addition of 110v input power supplies, an appropriate computer, and software would make a complete stand alone instrument, but it is assumed that most users are integrating the instrument into systems which already have power converters and computers. The concept instrument then, consists of the following:

- A sensor, consisting of a tapered element with collecting stage, optics, and driving plates, all in a housing with a wiring connector
- An analog circuit which powers the optics and senses through them the vibrating frequency of the tapered element, conditions and sends that frequency to the counter, and powers the electrostatic drive of the tapered element through a feedback circuit
- A frequency counter which counts in such a way that sequential short gate time frequency readings can be chained together without accumulating gating errors
- A precision clock for the counter to use

- A temperature controller which controls the temperature of the housing and tapered element

Figure 1 shows a demonstration system, which consists of all the above mentioned items plus a 110 v supply. A  $.01 \text{ cm}^2$ ,  $5 \times 10^{-12} \text{ g}$  resolution sensor assembly is in the foreground, removed from its heated sleeve. (Figure 2 shows the sensor in more detail). In the center is the analog circuit, with almost all flight qualified parts. The board itself is on the right, and the 110 v power supply, potted, is on the left. Balanced on the edge of the analog circuit case is one of R&P's commercial counter boards, with a temperature controlled crystal oscillator installed on the board as the clock. (A separate H P high precision clock was used for all data cited in this report.) The counter board was used in an IBM XT for this contract, but works in many other models and brands of personal computers. At the very top of the picture is a YSI model 72 temperature controller, a very fine proportional controller.

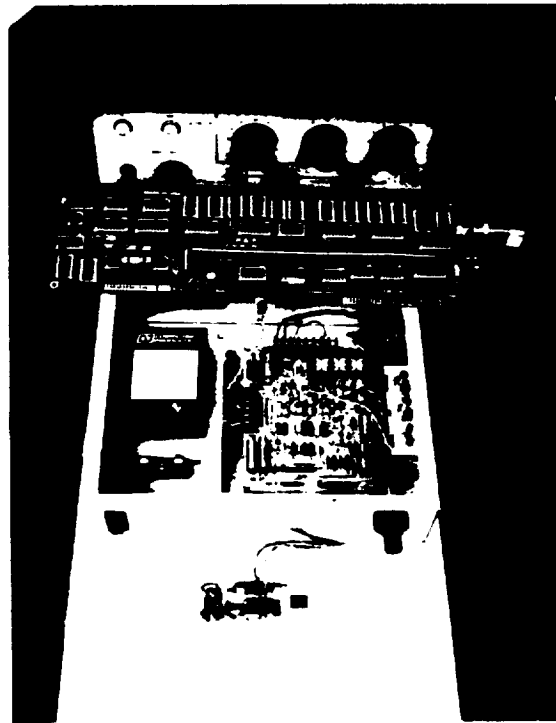


Figure 1. Portable Version of Concept Instrument

This system was put together as a demonstrator, so that everything could be tucked into a briefcase and taken to a potential user's lab for testing. With the addition of any IBM PC compatible computer and software, the system is ready to go in air or vacuum. The analog circuit is shown with potentiometers so that this one circuit can be used to run any size sensor. In a flight version, fixed resistors would be substituted. The only adjustment needed after initial setup is to adjust the drive amplitude when the sensor is moved from air to vacuum.

### 1.3 Sensor Descriptions

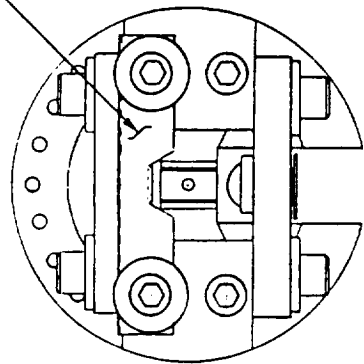
Figure 2 is the assembly drawing used to manufacture all three sizes of sensors. The only external difference between the three sizes of sensors is the size of the collection stage. Close examination would also show that the tapered elements of the high sensitivity sensors are a bit more slender near the stage. At the right of the drawing is a section sketch of a sensor installed in the JPL view limiter showing the position of the tapered element and its proportions.

Figure 3 is a top view of eight sensors mounted to a block for vibration testing. Not all the stages are visible, especially the silicon carbide medium and low which are transparent. Two round  $1 \text{ cm}^2$  beryllium stages are clear at center and lower left. A square  $.1 \text{ cm}^2$  single crystal silicon carbide stage has caught a strong reflection at center right. At top center a  $.01 \text{ cm}^2$  square silicon carbide stage is barely visible.

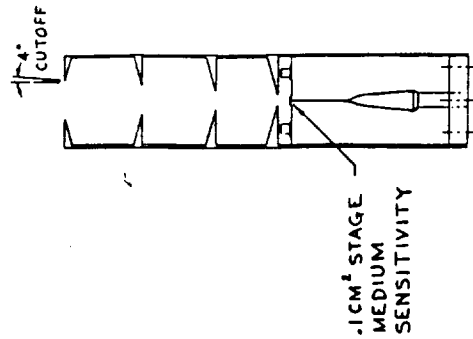
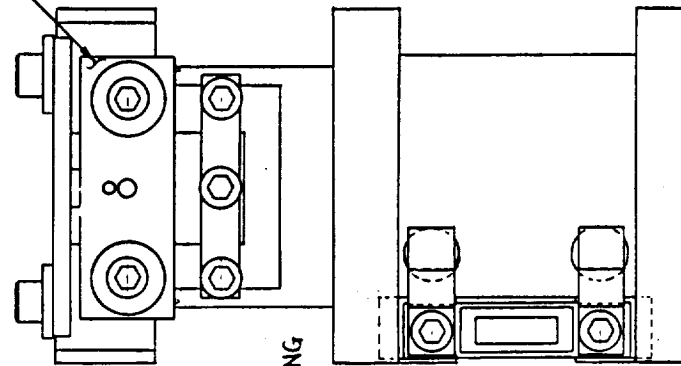
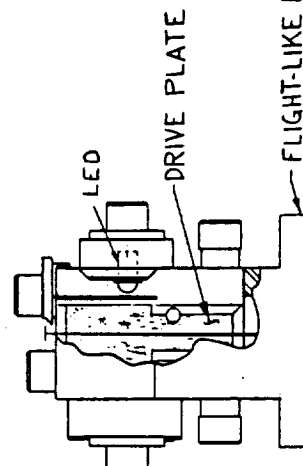
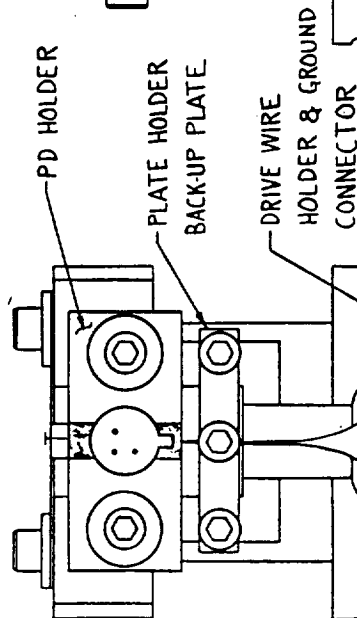
### 1.4 Principle of Operation

Figure 4 is a diagram of the tapered element and optics which comprise the essential parts of any TEOM<sup>®</sup> sensor. The tapered element is a hollow, elliptical tapered cantilever beam, rigidly clamped at one end, and free to oscillate at the other end. The free end has the collection stage attached. A narrow beam of infrared light passes the tapered element from the LED. The frequency of oscillation is detected by the action of the tapered element gradually blocking and unblocking the narrow light beam, resulting in a sinusoidal signal at the photodetector. This sinusoidal signal is amplified, shifted 90 degrees, and applied to a conductive coating on the tapered element. Field plates on either side of the tapered element produce a DC field, and the interaction of the AC voltage on the tapered element with the DC field produces a mechanical driving force to sustain oscillation of the tapered element.

LED SLIT

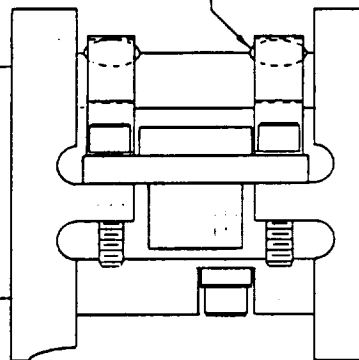


LED HOLDER



FLIGHT-LIKE HOUSING  
IN VIEW LIMITER

THERMISTOR



TE BASE

**RUPPRECHT & PATASHNICK CO., INC.**  
 6 CORPORATE CIRCLE, ALBANY NY 12203

ASSEMBLY - FLIGHT-LIKE HOUSING

DATE: 4-1-67  
 DRAWN BY: JFC  
 CHECKED BY: JFC  
 PART NO: 0020HEAD  
 REV: D

Figure 2. Assembly Drawing

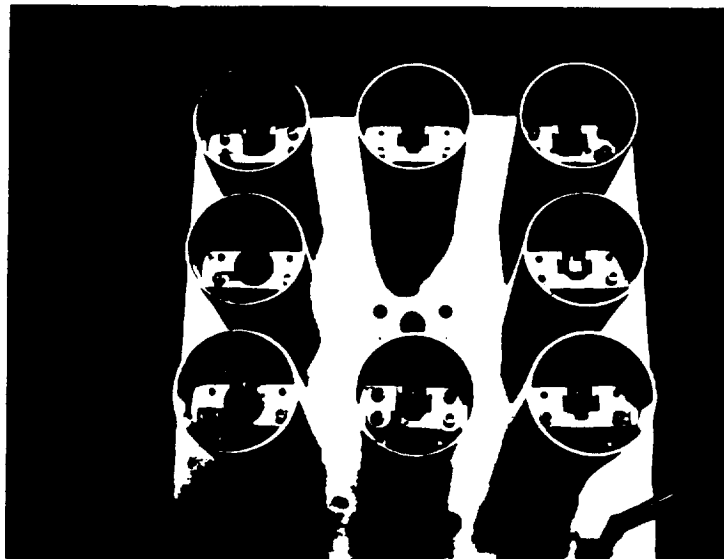


Figure 3. Eight Complete Mass Sensors

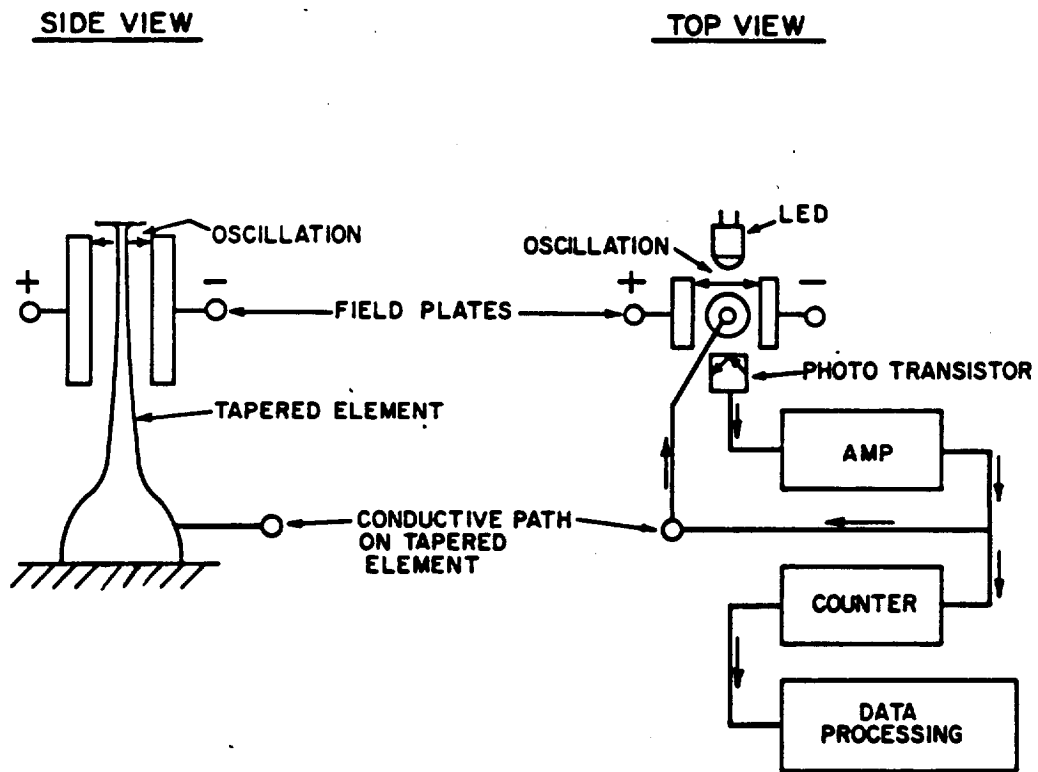


Figure 4. Sensor Operating Principle

The special shape of the element ensures that it will oscillate in only one plane and that higher mode frequencies are suppressed. The frequency of oscillation is that of a first order mass spring system, with the cantilever beam as the spring and the stage and collected material as the mass. As mass accumulates on the collecting stage, the frequency decreases. The permanent change in natural frequency of the sensor is measured to determine how much mass is accumulated. Time and mass resolution of the sensor are limited only by how often and how precisely the frequency measurements are made. Accumulation data is always available, even if the sensor has been turned off and the data stream interrupted, by virtue of the permanent change in natural frequency. This is a unique inherent reliability factor of the TEOM® sensor.

### 1.5 Data Reduction Methods, Sample Data

The equation of motion for the tapered element is

$$f^2 = K_0/m$$

$f$  is the natural frequency in hz  
 $m$  is the total oscillating mass in grams  
 $K_0$  is the spring constant divided  
 by  $4\pi^2$

The total oscillating mass is composed of three parts: the portion of the tapered element itself which is oscillating (effective mass), the collecting stage (including any sticky collection material on the stage) and the mass of any particle or particles collected. The total oscillating mass is divided into two parts for convenience:  $dm$ , the mass collected, and  $m_0$ , the mass of the element, stage, and collecting material. If the natural frequencies before and after a particle capture or mass accumulation are designated by  $f_1$  and  $f_2$ , then:

$$\begin{aligned} f_1^2 &= K_0/m_0 && \text{and} \\ f_2^2 &= K_0/m_0 + dm \\ &\text{or} \\ m_0 &= K_0/f_1^2 && \text{and} \\ m_0 + dm &= K_0/f_2^2 \end{aligned}$$

Subtracting and rearranging these equations yields:

$$dm = K_0(f_2^{-2} - f_1^{-2})$$

So if  $K_0$  and the frequencies before and after any event are known, the mass gain (or loss) due to the event is easily calculated. Note that  $m_0$  is not needed for mass gain or loss

calculations.  $K_0$  is determined by using the last equation and measuring frequency with and without a known calibration mass  $dm$  on the sensor. Careful study has shown that the TEOM® sensor has a huge range accurately represented by the simple equation above. A single calibration weight of any convenient size (even seven orders of magnitude larger than the resolution of the sensor) will suffice to determine  $K_0$  accurately.

Temperature of the tapered element and optics can also affect frequency. In the case of any single particle detection, the temperature change between frequency readings is usually so small as to be unimportant. High rates of change of temperature can lead to an erroneous evaluation of mass accumulation rate. Once the temperature stabilizes, however, one can make use of the fact that true mass accumulation makes a permanent change in natural frequency and correct the data. For long term (days, weeks or months) accumulation measurements where the starting and ending temperatures may be unavoidably quite different, a frequency correction can be calculated as long as these temperatures are accurately known. The correction equations will be discussed in section 4.1.4. The best way to use these sensors, however, is to keep them at a constant temperature. Ideally, everything should be kept between 20 and 40 deg C where the coefficient is very low. The absolute best results come from holding the whole sensor at 32.5 deg C, where the temperature coefficient of frequency is 0.

The output of the sensor and its related analog electronics circuit is a frequency which decreases as mass accumulates. A few words about frequency measurement is in order before presenting sample data. In its simplest form, a counter holds open a gate for a fixed time period and counts the number of whole cycles which pass through the gate. Obviously the gate timer (clock) stability and the rounding to whole cycles are sources of error. More sophisticated counters open the gate at the start of a cycle, hold it open for a fixed time and then keep it open until the last cycle completes. This scheme varies the "gate time" with each measurement. This increases the accuracy, and also increases the amount of data to be passed to the digital electronics, since both number of cycles and duration vary. This second type of counter is the type most often encountered. For this counter, assuming a good clock, the biggest error comes from the timing of the "zero cross", the beginning and end of the train of cycles. The error can arise from the zero cross detector, or from noise or distortion on the waveform being measured. The basic % of error is the sum of the timing errors in the first and last cycles divided by the gate time. The longer the gate time the better the accuracy, until clock stability takes over at very long gate times. One disadvantage of this second type of counter is that when it is set up for maximum accuracy, time resolution can be lost; if two particles fall

during one long gate time, there is no way to evaluate each one separately. A second disadvantage is that these counters take samples of the frequency being measured. Each frequency value is independent; in each the error in gate opening and closing times has no relation to the reading before or after.

A third, and possibly unique, way to count has been developed by R&P. The actual implementation is too complex to explain briefly, but the basic idea can be explained. It keeps a clock counter running at all times and records the beginning and ending times of groups of cycles roughly corresponding to the number of cycles in a more conventional counter's gate time. All cycles are counted, not just samples. Because no cycles are ever dropped, the extra duration assigned to one group of cycles by a distorted zero crossing will be matched by a shorter time on the next group, or vice versa. By itself, each reading is no different than the corresponding reading from the second type of counter. However, when two readings are combined, either by adding the cycle counts and clock counts from two readings before dividing to get frequency, or by just averaging the two calculated frequencies, the result is the same as if double the gate time were used. This can be extended to any "gate time" desired. Once the data has been recorded, the same data can be processed at several different "gate times" or "averaging times", which is a more descriptive term for this type of frequency counting. The usual procedure in reducing a typical data stream is to process it first at a very short averaging time to identify events, and then use longer and longer averaging times to sharpen the resolution of the results.

For the highest possible resolution, long averaging times can be used in such a way as to position the end of one average approximately at the point in time when a particle falls in the data stream, and start a new average with the particle in place. Other techniques also can be used, once chaining of data is possible. If resolution is being stretched to the limit and there is uncertainty as to when the particle falls, two or three data points can be omitted between the long averages so as not to average across a frequency shift. A uniform background drift due to temperature drift or accumulation of unresolvable material can be compensated for by using least square fits on data before and after an identified event, and then using the mass difference between the two lines at the time of the event to get an accurate mass change for the event. Frequency domain filtering was tried on some data and shows promise.

Difference techniques compare the current mass with a mass one or two averaging intervals in the past. Difference techniques are useful in the initial identification of small particles widely spaced in time in a long dataset. Particles appear as peaks on a difference plot instead of the steps found

on a normal plot of mass vs. time. The peak heights are fairly good approximations to particle mass, and any drift due to thermal effects or unresolvable particle deposition can be readily identified and quantified as an offset of the baseline of the difference plot.

Sample data:

Figure 5 is a simple plot of mass vs time using 20 second averaging time (frequencies were collected at 1.678 sec intervals). Simple inspection shows 7 obvious particles landing in the 30 minute period. From inspection, the approximate sizes are:

<u>No.</u>	<u>Time (min)</u>	<u>Mass (x 10<sup>-10</sup> g)</u>	
		<u>Fig. 5</u>	<u>Fig. 6 or 7</u>
1	5	2.2	2.25
2	9	1.0	.95
3	11	.5	.45
4	18	.2	-
5	19	1.9	-
6	20.5	.9	-
7	24	.2	.15

Table 1. Mass of Particles Shown in Figure 5

This data was taken on a .01 cm<sup>2</sup> sensitivity sensor, in vacuum, using an electrostatic dust thrower throwing glass microspheres.

Figure 6 is the same data processed using 80 second center weighted averaging, obtained by taking 60 second averages of the 20 second data. The effect of center weighting is to give the smoothing effects of 80 second averaging when no mass is depositing, but give sharper edges to events than straight 80 second averaging. Since the averaging is done off line, it can use values in the "future" as well as past, so that for example in the 80 second center weighted average just described, 80/1.6 = 50 data values are used to calculate each point, 25 from the past and 25 from the future, with the first and last six not counted as heavily as the others. Several changes occur with the longer averaging time. For the first particle, which had several minutes with no events before and after it, a much easier assessment of its mass can be made by reading from the flat lines before and after. Notice, however, that the slope of the transition from one level to the next is much less, an effect

which virtually erases the fourth and sixth particles, which were separated by only about a minute from the fifth, less than the averaging time. In the 20 second averaging, there are visible small plateaus near 19 and 20 minutes which are clearly times when no resolvable particles fell. These plateaus are missing in Figure 6.

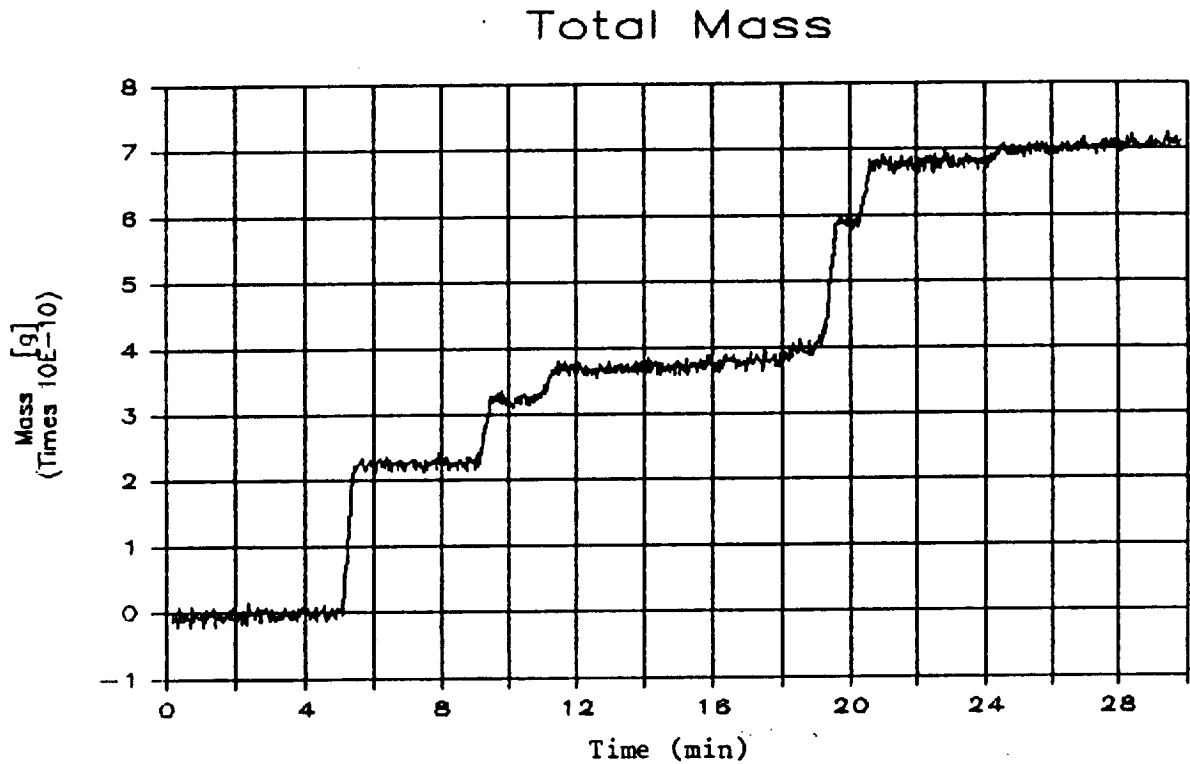


Figure 5. Seven Particles Landing on a  $.01 \text{ cm}^2$  Sensor, 20 Second Averaging

## Total Mass

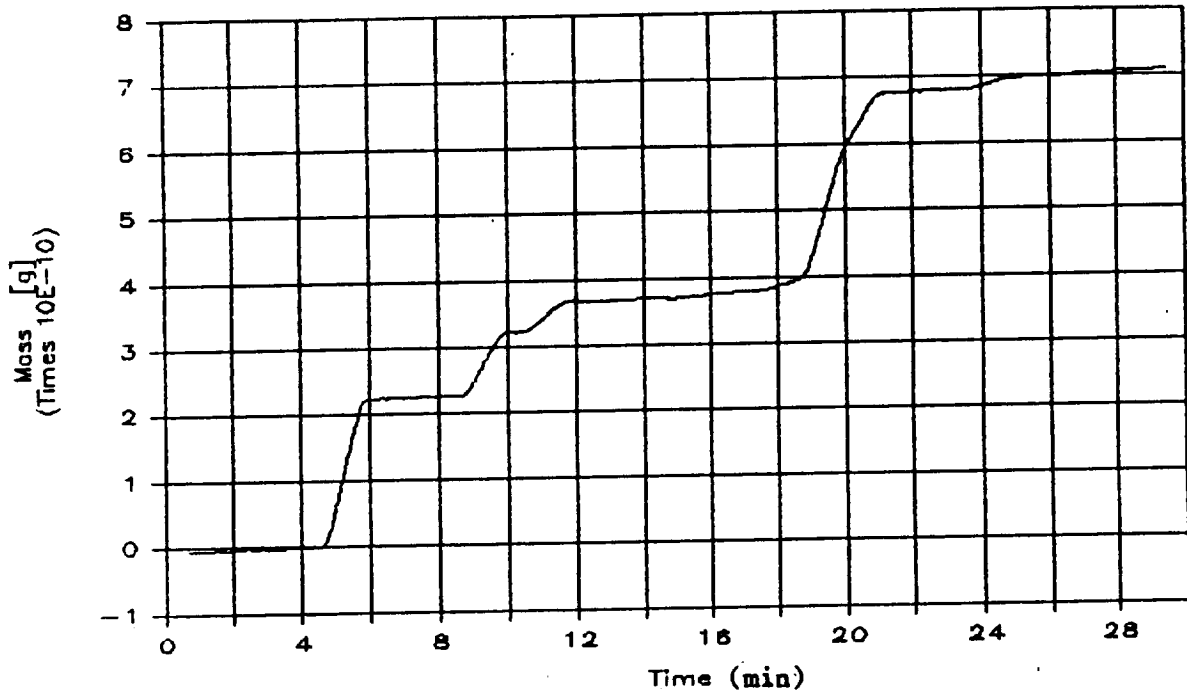


Figure 6. Seven Particles Landing on a  $.01 \text{ cm}^2$  Sensor, 80 Second Averaging

The conclusion of a comparison of averaging times is that ultimate resolution of a particular particle's mass depends on how often particles are landing and the relative sizes of the particles, as well as the basic noise and resolution numbers for a given sensor. One way to summarize this is shown as Figure 9, section 3.1, which shows the increase in resolution with averaging time, assuming that only one particle falls in any interval two averaging times long.

Figure 7 is a difference plot. Each point on Figure 7 is obtained by subtracting the value of a point 40 seconds ahead of the corresponding point on Figure 6 from the value of a point 40 seconds behind. The 80 second span of this mass difference looks across the smoothing of the data near the event to the undisturbed data on either side. It shows the time of occurrence and size of particles very clearly, if they land more than 80

seconds apart.

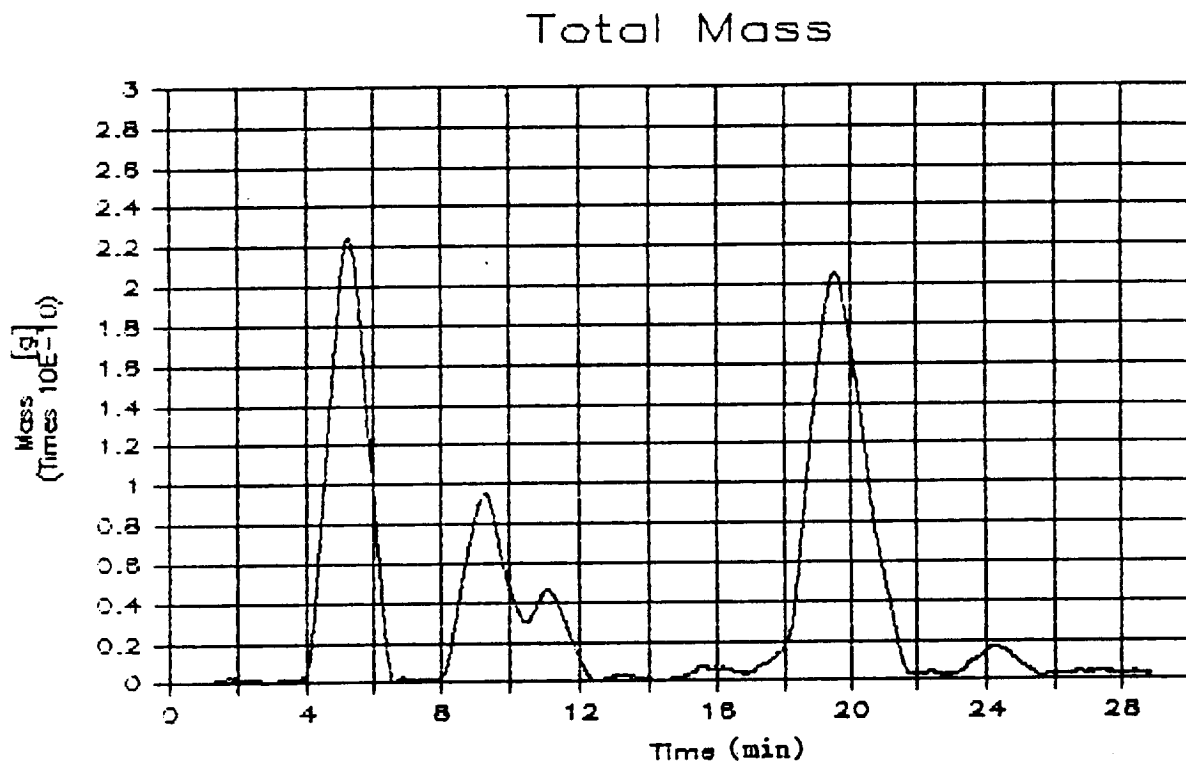


Figure 7. Seven Particles Landing, 80 Second Averaged Difference Plot

For times when the dust flux is not excessive, this type of plot and simple peak detecting software would very quickly and accurately classify particles and produce a good first cut mass distribution by particle size. Running the data at various averaging times and comparing the number and size of particles detected would quickly show whether the particles were adequately spaced to make good use of the high resolution available with long averaging times. In cases where long and short averaging difference plots give different numbers of particles, overlap is indicated and a close look at the short and long averaging time mass plots is warranted. A scheme such as this where the "easy" data is processed automatically at high resolution (projections for the CRAF mission are that maximum dust flux is less than one resolvable particle per 10 seconds) and the more difficult data is called to the operator's attention will be a great time saver when a large amount of data is to be processed. In any case the

mass plots always faithfully indicate true total mass, even if a high flux of particles prevents accurate separation of individual particles at the highest resolution.

Figure 8 shows, for a pair of particles not from Table 1, four possible ways of displaying the data, all superimposed on one graph. The rough stepped mass line and the rough, narrow peaks are 20 second averaged mass and difference plots, respectively. The smooth steps and smooth rounded peaks are 80 second data. Note the good agreement on the 20 second and 80 second difference peaks.

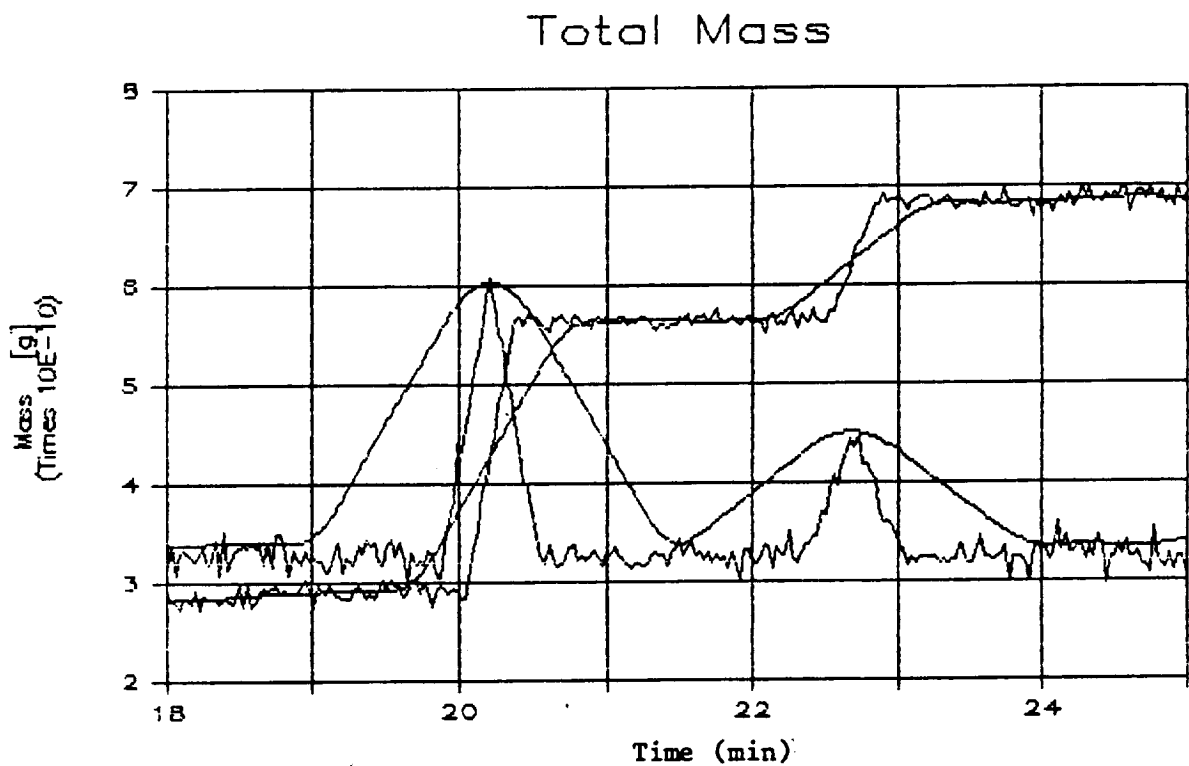


Figure 8. Two Particles, Shown by 20 Sec Ave, 80 Sec Ave, 20 Sec Difference, and 80 Sec Difference Plots

## 2. Scope and Task Description

### 2.1 Scope

Included in the scope of this contract was optimization and improvement of the high sensitivity sensors invented by R&P and later refined under JPL contracts and the first phase of this contract. Although a number of items are required to make a complete instrument, the tapered element is a key element and unique. Because of this uniqueness, the JPL and Phase I contracts were concerned almost exclusively with the tapered element part of the sensor. This contract extended that work, but also started to address other parts of a complete, flyable instrument. One major new area of emphasis was the optics system, which turns the physical motion of the tapered element into an electrical frequency signal. A search for rugged, small, flight approved parts and an arrangement which was easy to align and consumed little power was made an important part of the work. Another new area was analysis and redesign of the analog electronics board, which powers the optics, amplifies and phase shifts the drive signal, and filters and squares the output signal to the counter. The explicit charge was to reduce noise. Pursuing noise turned out to be a task which led to many other discoveries and improvements. Another new task was the development of a flight-like housing. The effort was directed at finding the smallest possible envelope for a sensor, sturdily mounting all necessary optics and drive hardware, and shaving weight wherever possible. The emphasis was on envelope and internal hardware mounting, since the overall structural strength and consequent weight will depend on how and where the sensor is attached to the instrument. The actual attachment was not a subject of this contract.

Two other areas broadened the scope of this work compared to previous work. Although quality control and quality assurance are always part of any design process, a new emphasis was put on designing and building the sensors in documentable and repeatable ways. The emphasis went from "does it perform?" to "can we make 10 like it and will they all survive and perform as well?". Testing assumed a new dimension. Up until this contract, the only weights the sensor saw were the large calibration weights, applied in air. This work included designing and building a facility to throw very small particles at the sensors and monitoring the dynamic behavior of a sensor in a flux of appropriate size particles.

Several areas were not within the scope of this contract, and should be pointed out. Although flight qualified parts were selected and used in the analog electronics work as much as

possible, very little consideration was given to connectors and packaging, except insofar as they affected the tests to be performed. Most of the work was done on plug in breadboards, and a printed circuit was made at the end only in anticipation of long term tests where soldered connections are more reliable. The analog board will be only a small one and should be made and mounted, including appropriate connectors, to interface well with the digital boards for the counter, clock, and microprocessor, other areas outside the scope of this work. All these areas have been addressed for R&P's commercial TEOM® systems, and indeed R&P's commercial counter, computer, and software were used to test these sensors. The flight versions of these components of a complete instrument will have to be radically different in size and power consumption. For the JPL comet dust application, JPL is addressing these components, as well as thermal management. The sensors' reaction to ambient temperature was extensively studied, but not the means of providing temperature control, since this is a part of overall spacecraft thermal management. Another area outside the scope of the contract is power supplies. The number of voltages and amount of power were kept to a minimum, and the sensitivity of the sensors to voltage fluctuations was studied, but no recommendations are given as to what type of supplies are to be used.

## 2.2 Contract Tasks

Enumerated here are the explicit tasks outlined in the contract, and a restatement where necessary to better identify the specific work needed to accomplish the stated goals. Restatements are in parenthesis.

- 1 Additional improvements and developments beyond those in phase one (lower power, higher sensitivity, better materials)
  - 1a Optimizing signal (study of optics, sensitivity analysis of photosensitive device and its driver circuit)
  - 1b Reduction of residual electrical noise (attention to cables and connectors, stability of drive circuit, signal levels and types, time constants, phase shifts and filter cut off frequencies)
  - 1c Evaluate and select a single glass type
- 2 Pilot production of (at least) 10 sensors
  - 2a Subject the units to simulated space conditions (high vacuum, temperature changes, dust flux)
  - 2b Expose components to stress and obtain failure mode

information (vibration tests: sweep, random, and single frequency; overload tests, pull tests on collection stages)

3 Develop and implement standardization of tapered element fabrication

3a Enable production of reproducible tapered elements (build computerized glassworking machine)

3b Develop fabrication processes to increase yield (primarily by replacing hand shaping and selection with a make to order process (see 3a): also upgrade annealing, coating and stage attachment equipment to give more predictable results)

3c Complete operational prototypes of (at least) one sensor of each size: 1, .1 and .01 cm<sup>2</sup>; sensors are to include all improvements from 1 and 2 above and comprise:

3c (i) Glass tapered element with flight-like base and stage (vibration tested, vacuum compatible, and tested for noise and resolution)

3c (ii) Housing representative in form (envelope) and function (containing all necessary elements and provisions for mounting and adjusting those elements) of spaceflight units

3c (iii) Optimized optical assembly

4 Establish and implement a quality control program for the production of tapered elements (tapered elements only: since flight electronics and housings will probably be made by others, their quality control programs will be used in production of those items. Installation and adjustment of the tapered element in a housing is included, however.)

5 Develop instrumentation to produce a particulate flux in vacuum and test sensors in that flux

6 Provide quarterly (monthly reports were actually used) reports and a final report

### 3. Objectives

In this section the objectives of the current work will be described along with recommendations as to how flight sensors should be specified and tested.

### 3.1 Performance, Sensor Specifications

The primary performance criterion is resolution at a given averaging time. The goals used varied as capabilities improved and as new information, such as that from Giotto, better defined the mass distribution of the particle flux likely to be encountered. Theoretically, a vanishingly thin tapered element with a collection stage of submicron thickness and area barely visible to the naked eye could determine the mass of .1 micron or smaller diameter particles. This is to say that there is no theoretical lower limit to TEOM® sensor resolution, only practical limits governed mostly by required collection area. Performance of any TEOM® sensor is a tradeoff between sturdiness and ease of assembly, on the one hand, and sensitivity and resolution on the other. The primary action of a TEOM® sensor is to translate a percent change in mass on the end of the tapered element into a directly proportional percent change in frequency. The formula, for small changes in mass, is:

$$\text{change in mass/total mass} = -2(\text{change in freq/base freq})$$

The smaller the total mass is, the larger will be the change in frequency for a given change in mass and the easier it will be to detect that frequency change. The majority of the oscillating mass in a sensor is in the collection stage. The stage must be selected for ease in reliable fabrication and attachment as well as low mass, and for this reason minimum thicknesses were arrived at for the beryllium and single crystal silicon carbide used for stages. Since the collecting stage areas are calculated to give statistically representative samples of different sizes of dust, and hence fixed, the stage masses are fixed by the minimum thickness and area thus arrived at. With only minor variations from size to size and sensor to sensor, the ability to resolve frequency is fairly constant for any given averaging time. Two canceling effects come into play. Larger sensor stages tend to introduce a bit more noise than small ones, but for large stages proportionately less mass is needed for the tapered element and attachment materials. In consideration of all the above and the experimental results to be presented later, these are the minimum resolution specifications to which any flight sensors can be expected to adhere, and constitute the main design objectives:

Collecting Area, shape	Total Oscillating Mass, $m_0$	Resolution (1 STD DEV)	
		20 sec ave	80 sec ave
1 cm <sup>2</sup> , round	$3.5 \times 10^{-3}$ g	$5 \times 10^{-10}$ g	$1.5 \times 10^{-10}$ g
.1 cm <sup>2</sup> , square	$5 \times 10^{-4}$ g	$5 \times 10^{-11}$ g	$1.5 \times 10^{-11}$ g
.01 cm <sup>2</sup> , square	$6 \times 10^{-5}$ g	$5 \times 10^{-12}$ g	$1.5 \times 10^{-12}$ g

Any counter and clock selected or designed for use with these sensors would of course have to support these resolutions per the equation mentioned above. Specifically, for the given  $m_0$ 's, the counter would have to maintain its noise level (expressed as delta freq/base freq:  $df/f$ ) below  $4 \times 10^{-8}$  hz/hz at 20 seconds and  $1.25 \times 10^{-8}$  hz/hz at 80 seconds for the .01 cm<sup>2</sup> sensor, which has the most stringent counter requirement because of its higher mass per unit area.

Figure 9 is a mass resolution vs averaging time plot for actual data taken on a .01 cm<sup>2</sup> sensor. It shows better resolution at 20 and 80 seconds than the table above. This is to be expected, since the tables show minimum values taking all the allowable variations in construction and alignment into account.

Other performance criteria include the ability to accept a large mass accumulation and still function. Performance in the face of a hostile environment, including vibration and temperature extremes, is also important, as well as the effects of small temperature changes on frequency.

The dust accumulation for the CRAF mission is not expected to exceed two monolayers (2 milligrams per cm<sup>2</sup>) which is less than 2/3 of one additional  $m_0$  for any given sensor. The effects of the accumulated mass are several. First, once more than 1 monolayer of dust is collected, one must rely on the sticky layer to encapsulate the dust and keep a sticky surface presented to space. This was seen to occur in tests conducted by Dr. Ben Clark of Martin Marietta Corporation several years back; in any case the other experiments on board, especially those with optics, want to limit total exposure to no more than one or two layers of dust. The second effect is the same as if a heavier stage were used. Doubling the oscillating mass halves the frequency change to be expected from an increment of mass accumulation. Therefore, expected resolution would be expected to drop by less than a factor of two if less than 1  $m_0$  of total accumulation occurs. A reasonable objective and test for flight units would be application of a single load 5x the

## MASS NOISE vs. AVERAGING TIME

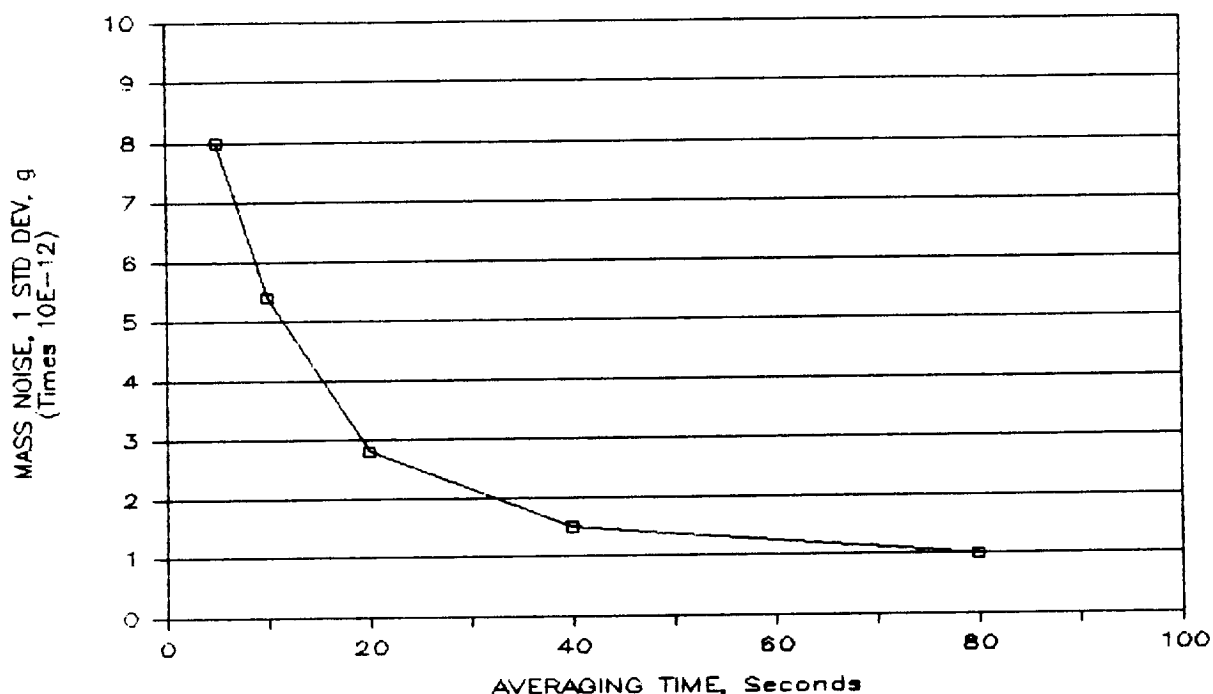


Figure 9. Averaging Time vs Resolution, .01 cm<sup>2</sup> Sensor

maximum anticipated mission load and comparing the resolution and electronics performance at 0 load and 5x mission load. This would also be helpful in selecting the best initial gain settings for the electronics.

Launch vibration was addressed by testing sensors for survival using random and swept vibration per the most recent available information from CRAF. These test specifications will probably be updated and of course any other application will have its own test specifications, so actual test specifications used will not be belabored here. (Some additional information will be found in the Results section and in the Appendix on vibration test results.) In anticipation of different specifications and other applications, the sensors were also subjected to much higher g level sweeps at their most vulnerable frequencies and even to single frequency unswept inputs at their primary and secondary (cross direction) frequencies, in order to try and find failure modes. No failures could be induced, even in sensors which would

probably have been rejected on workmanship grounds for having incomplete fusing in the stage attachments. In view of these results and others detailed in the Results section, no vibration or stress tests beyond the launch sweep and random tests are indicated.

Absolute temperature limits of the sensors are set by the flight approved LED's, which have operating limits of -65 to +125 deg C. The tapered elements including the aluminum bases see temperatures higher than 400 deg C in many stages of assembly, so there are no high temperature problems with them. When complete sensors are baked out prior to being put in vacuum, 100 deg C is used. The CRAF environmental requirement for non bus mounted equipment is -45 deg C to +100 deg C with a 10 degree design margin. One sensor has been subject to -55 deg C. The only possible problems with low temperature would be loosening of the shrink fit on the base or cracking of the glass-metal interface. Generous design margins were used in these areas and confirmed by the sensor surviving this test intact. Extreme high and low temperature testing of sensors by themselves is probably not useful.

It will be noticed that nowhere in this report is a complete set of hard and fast specifications. This is not an accident. It is hoped that those who wish to use these sensors in a particular application will take the time to study both the capabilities and necessary tradeoffs and then formulate their own set of performance specifications which customize the collection area, power, resolution, etc. to best match the needs of a particular application. The goal of this project was not just to make three "take it or leave it" products. The goal was to develop design and manufacturing capabilities for a wide range of sensors and demonstrate that capability through production of three prototypes suitable for the CRAF Mission. For example, there is no reason why a .2 cm<sup>2</sup> version could not be made, or a 2 cm<sup>2</sup> one, as long as the tradeoff between m<sub>0</sub> and resolution is understood. Similarly, for earthbound or orbital applications where power and weight limitations are not as severe, there are some power and weight intensive ways to increase resolution or loading capability of a given sensor.

### 3.2 Manufacturability

The prime requirement here was defining both process and machinery for making repeatable tapered elements. Although the quality and durability of hand made tapered elements has been high, they are not at all repeatable when small ones are made by hand. A computer controlled "puller" was to be designed and built to R&P's specifications. Similarly, the annealing and coating operations, conducted at temperatures over 600 deg C, and the stage attachment operation, conducted at over 800 deg C,

needed to have good controls and repeatable temperature profiles on heatup and cooldown. This equipment would be a minimum requirement to make even flight prototype units.

Another major manufacturability issue was the optics system. Required was a system which was efficient enough to require less than 5 ma for the LED, but at the same time compact and simple enough to give confidence that alignment could be maintained over the many years of the flight. As will be detailed in the Results section, this led from various types of lens systems back to a low power version of R&P's tried and true slit optics system. The extra sophistication went into the circuit powering and detecting the photosensitive device, rather than in trying to manhandle the infrared light beam into a tightly focused and hard to align spot. It is strongly recommended that any reintroduction of the various lens and mirror arrangements proposed in years past be avoided in flight sensors. The choice of optics system was made primarily on the basis of manufacturability and reliability.

The final manufacturability issue is the housing. The housing as it presently exists probably has too many small parts. This is as a result of trying to maintain some flexibility in mounting the drive plates and optics since the housings (8 were eventually made) had to be designed and built before the vibration tests could be run, and yet the results of the tests could have caused changes in the housing design. In the end, the design was not changed. In any case, once the first physical mockup of a particular space instrument is made, decisions will have to be made such as whether the housing supports the viewlimiter or vice-versa and where the connector should be located. Once these decisions are made, the basic external structure of the housing will be easier to define and many of the small parts now used can probably be consolidated. The materials used are aluminum for the basic structure; copper clad PTFE circuit board for the drive plates, drive wire support, LED mounting, and Photodarlington mounting; stainless steel cap screws; brass for the slit; and a plastic bodied electrical connector with teflon insulated wires. Two material changes are recommended for flight. A glass and metal or ceramic body is recommended for the connector. One connector body shed a few small pieces and another cracked at a mounting ear when subject to high temperatures for a long time in vacuum. It caused no problems in the work done, but would not be acceptable for flight. Brass is perhaps not the best material for the slit, as it may form a dusting type corrosion in storage or from handling. The flight version could be stainless steel to better survive all the handling and inspections required for a flight qualified parts manufacturing effort.

### 3.3 Quality Control

#### 3.3.1 Influence of Quality Control Considerations on Design

The quality control task was introduced early in the design work, in that designs and processes which resulted in a functional product only through selection or testing were rejected in favor of designs which could be implemented in such a way that control of fabrication at each step resulted in high yield and orderly progress to the next fixed step. Formerly, hand made tapered elements had been made in large batches of varying size elements and usually only 2 or 3 of a dozen were suitable for processing into final product. Even those which were suitable usually had wide variations in wall thickness and ellipticity so that subsequent stage attachment procedures, for example, had to be adapted to each tapered element individually.

The first Quality Control task was thus to analyze some of the best hand made tapered elements, measure and test them, and design manufacturing processes which could reproduce them one after another. The analysis and sectioning of the hand made tapered elements also identified any weak points, such as thin wall sections near the base which were designed out of the machine made ones. Analysis also included formulation of a computer model of the tapered elements, taking into account length, wall thickness, ellipticity and major and minor diameters. The model predicted  $m_0$ 's,  $K_0$ 's and operating frequency from the above dimensions and known physical properties of the glass. The model was used to balance requirements such as heavy wall thickness for easy stage attachment with conflicting requirements such as low  $m_0$ . The hundreds of trials needed to keep  $m_0$ , ellipticity, frequency and length in the right ranges and at the same time maintain sufficient diameter and wall thickness for good stage attachment were done in hours on the computer instead of the months which experimenting would have taken. Periodically a computerized puller-made tapered element was sectioned and its dimensions plugged into the model to help refine the model and assure its predictive value. Thus the machine made tapered elements are not just repeatable versions of the handmade ones, but engineered items with known, controlled, and balanced dimensions. They are balanced to maximize the strength and noise rejection properties inherent in the patented elliptical tapered hollow section, and to provide a sturdy and predictable attachment geometry for the stage.

All the dimensions and derived values mentioned above are nondestructively measurable in the final product except wall thickness. The manufacturing process was arranged, however, so that there are pauses in the pulling program when samples can be

removed from the process and sectioned before much value has been added or time spent on them. Examination of samples can confirm that wall thickness decreases smoothly from the base to tip. The sample can be snapped into short lengths and the sections examined side by side under a microscope. The diameters, wall thickness, and ellipticity at the working end of every tapered element is checked by examination of a similar, short length removed during frequency adjustment.

### 3.3.2 Inspection points

A list of inspection points for tapered element construction and installation is given here, extracted from the detailed discussion of manufacturing and quality control in the Results section. It can serve as a checklist for specifying inspections of flight sensors. It is in more or less chronological order to the actual construction process.

<u>Item</u>	<u>Use</u>	<u>Procedure</u>
Commercial Kovar tube to glass tube transition	TE base	Inspect for cracks, check dimensions, seal quality
Special tube from Corning	TE body	Inspect and mark for removal any bubbles or inclusions, check dim's
TE blank (assembled from above parts)	TE	Inspect for cracks at glass-metal and glass-glass joint, check dim's, clean
TE puller	Glassworking	Check vacuum level, program, filament alignment
TE after first operation	TE	Check for round ID
TE after second operation	TE	Check for ellip ID and check length
TE after third operation	TE	Check length, all dim's of tip
Annealing/coating furnace	1st coating	Check program, use proper Plat sol'n
Annealing/coating furnace	2nd coating	Check program temp's, use proper gold soln's
Calibration fixture	$m_o$ & $K_o$ determination	Clean & grease calib wt use proper program
SiC xtal or Be foil	TE stage	Check dim's, examine in cross light for cracks
Glass shard (ball)	Bonding stage	Weigh or measure, check for proper type
Kovar disk (Be stage only)	Bonding stage	Clean, check for flat glass surface after

Catalytic cure polyester	Bonding Be	acid removal of Kovar Blend and thin properly, dry and heat seal at proper temps
TE stage bonder	Glassworking	Check settings on controller, clean titanium surface of hotplate
Bonded stage	TE	Check for straightness of TE tip, complete fusion of tip into ball, check footprint of ball
Solder & wire	TE contact	Use proper soldering temp, clean well after
Shrink hotplate & aluminum disk	TE base	Measure for interference fit, set proper temp, calc spacers to put stage at proper height
Finished TE	Sensor	Repeat calibration as above, check $K_0$ , $m_0$ , freq, cross freq, length
Housing (TE installed)	Sensor	Check dim's, wiring, signal level, physical amplitude, LED & PD currents

#### 4. Results

##### 4.1 Performance

The principles of operation and data reduction have been fully explained in the previous sections. This section will only present the particular data sets and calculations which were used to draw the conclusions presented in previous sections.

##### 4.1.1 Resolution

Figures 10 through 15 show short term background noise (zero stability) plots for each size of sensor. These plots (and many others like them) are the basis for the nominal resolution values cited in section 3.1.

Figure 10 is a 1500 sec (25 minute) duration recording of 20 second averaged mass data from a .01 cm<sup>2</sup> sensor, number 930. The sensor had been in vacuum for 3 days. Data points were collected each 3.3554432 seconds (2<sup>25</sup> counts of a 10 Mhz clock), and a running average (6 values) is used to get "20 second" average values. The standard deviation of all mass values in the 25 minute period is  $3.05 \times 10^{-12}$  g. At this averaging time no

monotonic drift is apparent, so no correction of the standard deviation was made for drift.

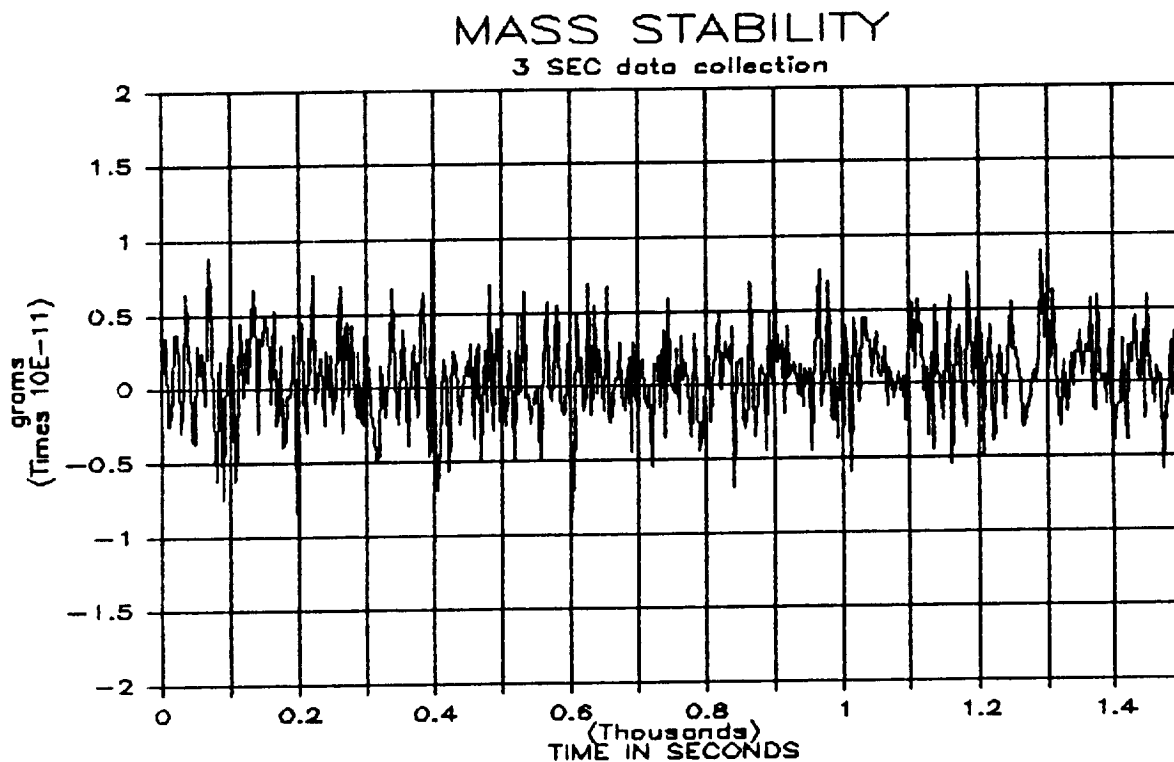


Figure 10. Resolution at 20 Second Averaging,  
.01 cm<sup>2</sup> Sensor  
Std dev  $3.0 \times 10^{-12}$  g

The conditions of running were nominal:

LED current:	5 ma
PD current:	.22 ma
PD driver output:	3 VAC P-P
Drive voltage:	40 VAC P-P
Plate voltages:	+15 VDC, -32 VDC
$k_0$ :	2.63
$m_0$ :	$5.8 \times 10^{-5}$ grams
Temp:	32.50 deg C
Vacuum:	$5.3 \times 10^{-7}$ torr (Ion pump)

The raw 3 second points were re-averaged off line to a running average of 80 seconds (24 values). The standard deviation of the 80 second averaged values is  $9.72 \times 10^{-13}g$  and the data is plotted as Figure 11.

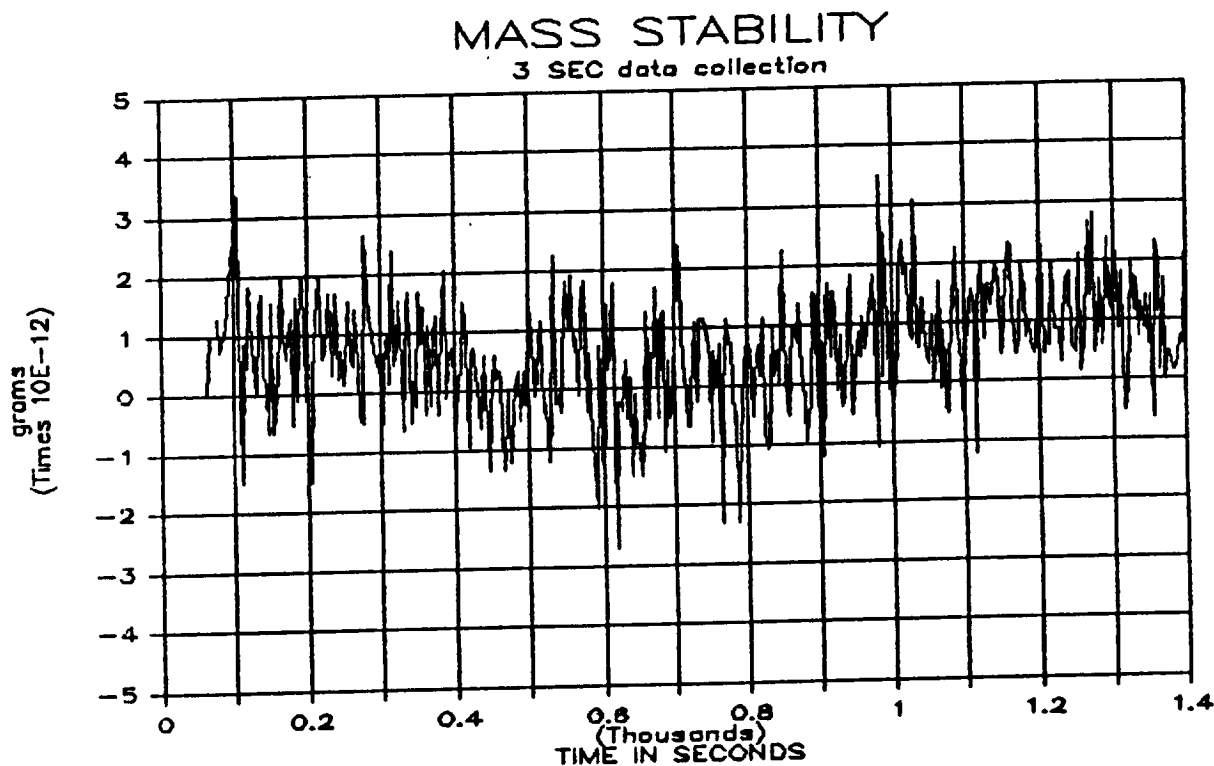


Figure 11. Resolution at 80 Second Averaging,  
.01 cm<sup>2</sup> Sensor  
Std dev  $9.7 \times 10^{-13} g$

Figure 12 is a 1200 sec (20 minute) duration recording of 20 second averaged mass data from a .1 cm<sup>2</sup> sensor, number 934. The sensor had been in vacuum for 3 days. Data points were collected each 3.3554432 seconds (2<sup>25</sup> counts of a 10 Mhz clock), and a running average (6 values) is used to get "20 second" average values. The standard deviation of all mass values in the 20 minute period is  $1.4 \times 10^{-11} g$ . At this averaging time no monotonic drift is apparent, so no correction of the standard deviation was made for drift.

# MASS STABILITY

3 SEC data collection

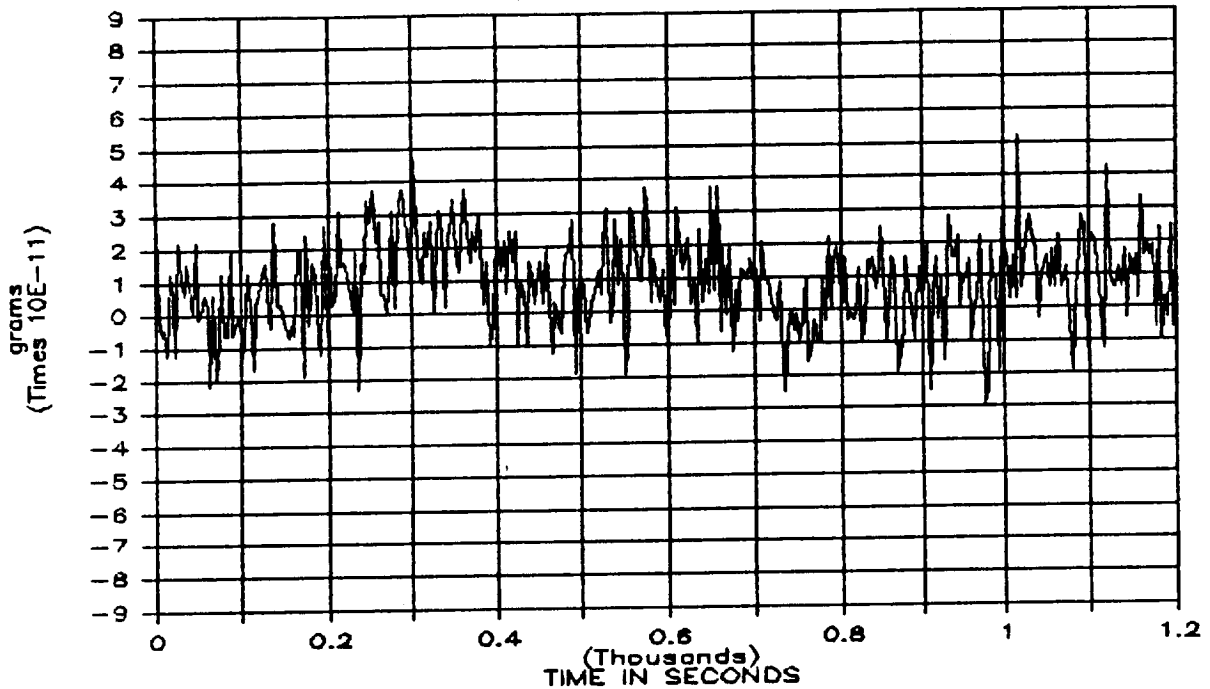


Figure 12. Resolution at 20 Second Averaging,  
 .1 cm<sup>2</sup> Sensor  
 Std dev  $1.4 \times 10^{-11}$  g

The conditions of running were nominal:

LED current:	5 ma
PD current:	.3 ma
PD driver output:	3 VAC P-P
Drive voltage:	50 VAC rms
Plate voltages:	+15 VDC, -83 VDC
K <sub>0</sub>	22.1
m <sub>0</sub>	$3.7 \times 10^{-4}$ grams
Temp:	32.50 deg C
Vacuum:	$2.5 \times 10^{-7}$ torr (Ion pump)

The raw 3 second points were re-averaged off line to a running average of 80 seconds (24 values). The standard deviation of the 80 second averaged values is  $6.6 \times 10^{-12}$  g and the data is plotted as Figure 13.

# MASS STABILITY

3 SEC data collection

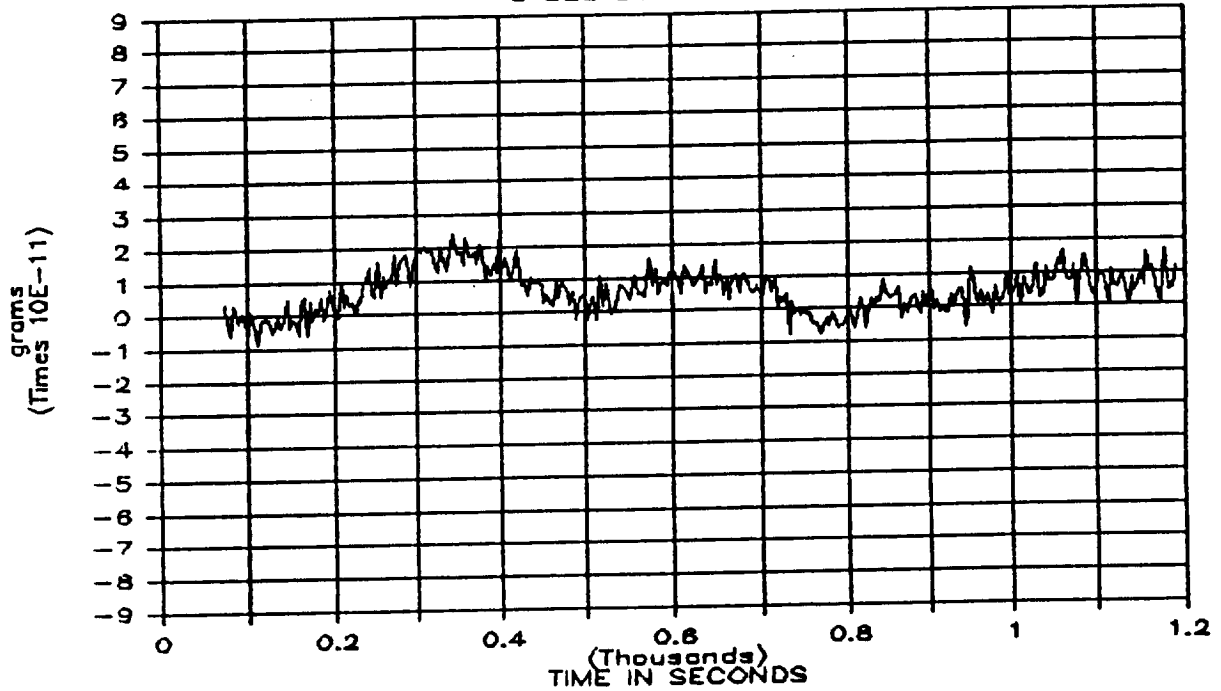


Figure 13. Resolution at 80 Second Averaging,  
 .1 cm<sup>2</sup> Sensor  
 Std dev  $6.6 \times 10^{-12}$  g

Figure 14 is a 1300 sec (21 minute) duration recording of 20 second averaged mass data from a 1 cm<sup>2</sup> sensor, number 927. The sensor had been in vacuum for 4 days. Data points were collected each 3.3554432 seconds ( $2^{25}$  counts of a 10 Mhz clock), and a running average (6 values) is used to get "20 second" average values. The standard deviation of all mass values in the 21 minute period is  $1.82 \times 10^{-10}$  g. At this averaging time no monotonic drift is apparent, so no correction of the standard deviation was made for drift.

# MASS STABILITY

3 SEC data collection

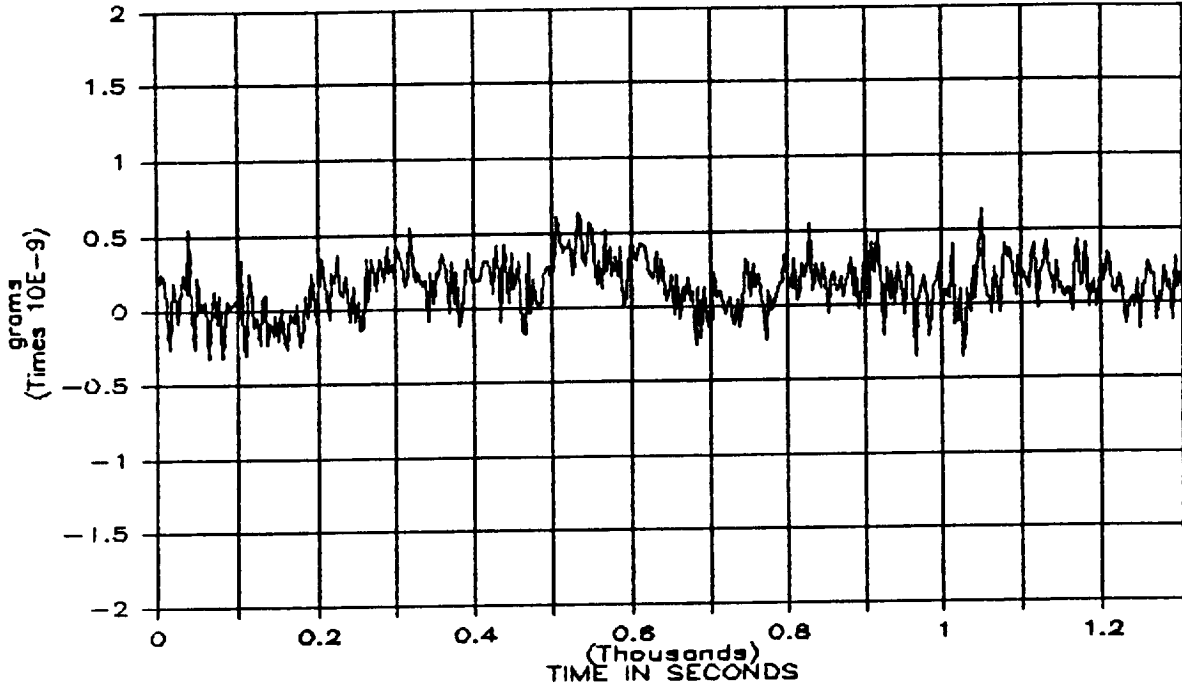


Figure 14. Resolution at 20 Second Averaging,  
1 cm<sup>2</sup> Sensor  
Std dev 1.8 x 10<sup>-10</sup> g

The conditions of running were nominal:

LED current:	5 ma
PD current:	.133 ma
PD driver output:	3 VAC P-P
Drive voltage:	127 VAC rms
Plate voltages:	+15 VDC, -185 VDC
K <sub>o</sub>	161
m <sub>o</sub>	3.0 x 10 <sup>-3</sup> grams
Temp:	32.50 deg_C
Vacuum:	5.3 x 10 <sup>-7</sup> torr (Ion pump)

The raw 3 second points were re-averaged off line to a running average of 80 seconds (24 values). The standard deviation of the 80 second averaged values is 1.06 x 10<sup>-10</sup> g and the data is plotted as Figure 15.

# MASS STABILITY

3 SEC data collection

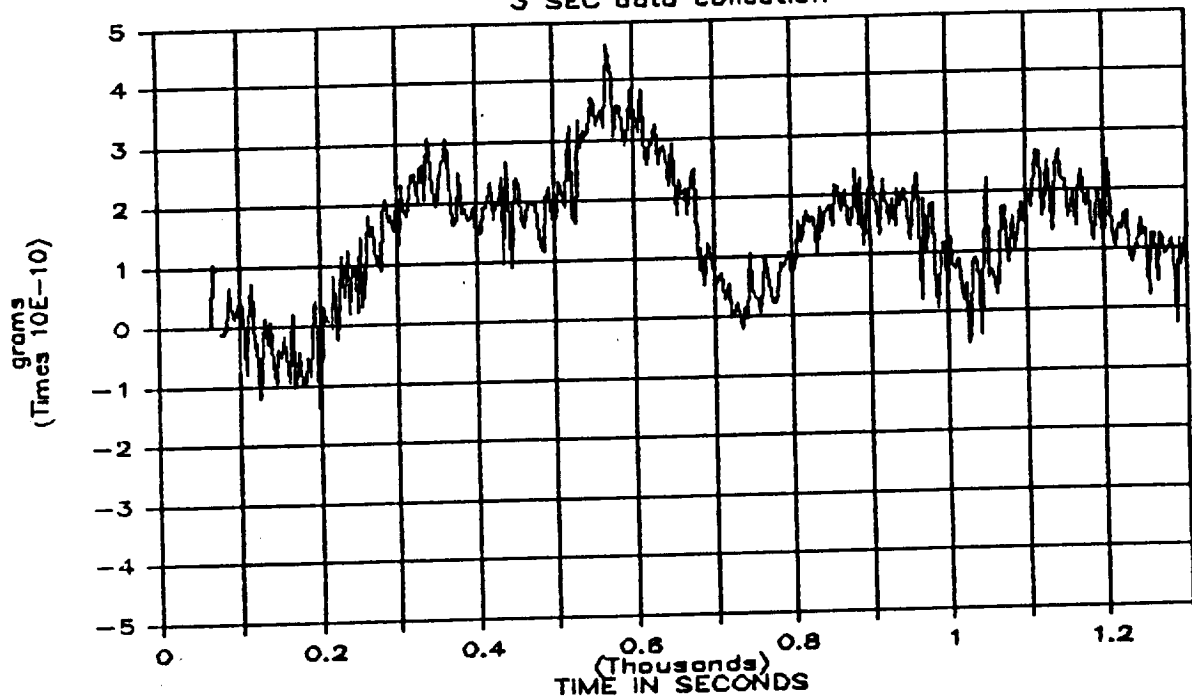


Figure 15. Resolution at 80 Second Averaging,  
1 cm<sup>2</sup> Sensor  
Std dev  $1.1 \times 10^{-10}$  g

## 4.1.2 Stability (Drift)

Drift is defined for the purposes of this discussion to be indicated accumulation or loss of mass when the sensor is in vacuum and no mass is being intentionally added or removed from the sensor collecting stage. In theory there can be many causes for an apparent mass loss or gain. All of these causes have one thing in common; they result in a real frequency change.

The most obvious cause of drift is real mass loss caused by evaporation of surface deposits of water and oils not removed in cleaning and vacuum bakeout. In addition to materials not removed during cleaning, there is the possibility of contamination during the rough pumping of the vacuum chamber when oil could backstream through the trap and deposit on the tapered element. Material present through either one of these mechanisms would slowly evaporate away once the chamber is sealed off and the ion

pump is on. If contamination were the prime source of drift, one would expect to see the rate of loss decrease with time, as the contamination was depleted. All data for all size sensors shows rapid decrease in rate of mass loss for at least the first week in vacuum.

If contamination were the primary cause of drift, removing the stage should decrease the area available for deposit and decrease the drift rate. Sensor #501, with a tip diameter of just 2 mils, was put into vacuum without a stage (this reduces the area in motion by about 8x) and run for several weeks. For the last 10 days the loss rate was below  $1 \times 10^{-13}$  g/hr. Similarly, the loss rate of #602, a .1 cm<sup>2</sup> sized sensor without a stage, dropped to  $8 \times 10^{-13}$  g/hr after 2 weeks. These drift rates are 40 to 50 times less than those of elements with stages, showing the strong dependence of drift on stage area.

Other possible sources of drift include aging of the electronics, power supply drift, clock drift, temperature controller drift, and fatigue of the oscillating element. If all these effects combined don't amount to more than the numbers cited above, they aren't very important. All the above mentioned items were designed and/or selected to contribute less than  $10^{-14}$  g/hr to the highest resolution sensor. The no-stage tests confirm proper design and selection. Similar selection rigor should be applied when mating these sensors into support systems which contain space qualified power supplies, a clock, and temperature sensing/control.

It is very difficult to get a "pure" drift experiment, as this ties up the vacuum chamber, sensor, and amplifier for extended periods. The usual procedure for sensors with stages was to run amplifier, temperature, and other tests during the day and collect drift data overnight. Ignoring the first few hours of data if temperature had to settle, at least 12 hours of undisturbed drift data could be had each night. Several days of good data was available over most weekends.

Sensor #606, with a .01 cm<sup>2</sup> stage, had a drift rate of  $-1.5 \times 10^{-11}$  g/hr after about a week in vacuum and dropped to  $5 \times 10^{-12}$  g/hr in another week. This was in a diffusion pump vacuum system. Sensor #930, with a .01 cm<sup>2</sup> stage was cleaned more carefully than sensor #606 and placed in an ion pumped vacuum system. After a few days the vacuum settled to  $5 \times 10^{-7}$  torr and the loss rate dropped to less than  $5.6 \times 10^{-12}$  g/hr. Sensor #923, with a .1 cm<sup>2</sup> stage, had a drift rate of  $-3.3 \times 10^{-11}$  g/hr after only a few days at  $5 \times 10^{-7}$  torr in an ion pump vacuum system. See Figure 16 for an example of drift data.

TE# 923, Med Sens, Final form  
Long term drift, 5 min data

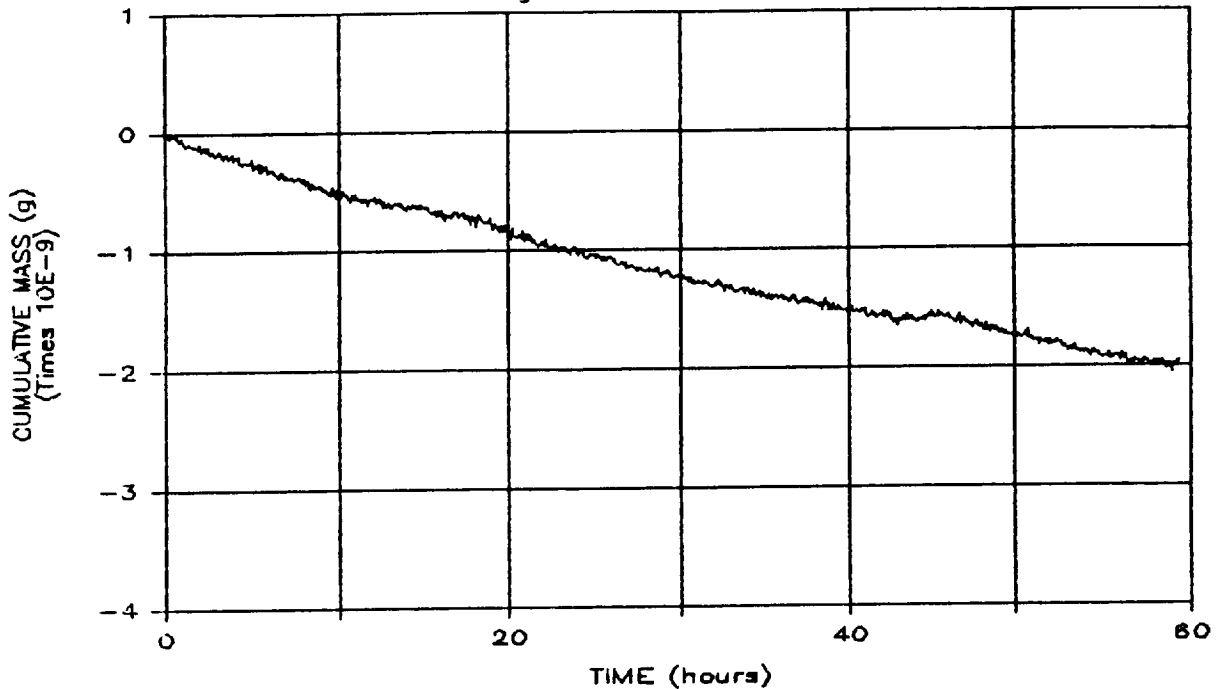


Figure 16. Drift of .1 cm<sup>2</sup> Sensor  
over Several Days  
Rate  $-3.3 \times 10^{-11}$  g/hr

Sensor #927, with a 1 cm<sup>2</sup> stage, had a drift rate of  $-2 \times 10^{-10}$  g/hr after 10 days in an ion pump vacuum system. The initial rate was somewhat higher than expected and may reflect the use of a catalytic cure, solventless polyester adhesive to attach the stage. Perhaps the polyester outgassed part of its original constituents, especially from the small amount of excess outside the actual joint. More likely, it absorbed some of the Freon used for cleaning and released it. The loss rate was still decreasing after 13 days.

#### 4.1.3 Dynamic range

Several factors determine the dynamic range of the sensors. First is the frequency capability of the analog electronics. As operating frequency goes lower, as it does when mass is added, eventually it goes below the design cutoff

frequency of the output transformer and below the linear region of integrator operation. Both items have been designed with a 100 hz lower limit to linear operation. As operating frequency goes higher (i.e. extending range by using a higher starting, or unloaded, frequency), more voltage is needed to drive the tapered element. This means a higher turns ratio and more weight in the output voltage step-up transformer. The turns ratio has been selected to allow 300 hz as a starting frequency. Using the delta mass equation from section 1.5:  $dm = K_0(f_2^{-2} - f_1^{-2})$ , the load limits due to frequency are as follows:

SENSOR SIZE	TYP $K_0$	MAX LOAD (dm) (300 to 100 hz)	DYNAMIC RANGE (dm/20 sec res)
.01 cm <sup>2</sup> sensor:	3	$2.6 \times 10^{-4}$ g	$5.2 \times 10^7$
.1 cm <sup>2</sup> sensor:	20	$1.8 \times 10^{-3}$ g	$3.6 \times 10^7$
1 cm <sup>2</sup> sensor:	160	$1.4 \times 10^{-2}$ g	$2.8 \times 10^7$

Other factors come into play before these limits are reached. Each monolayer of collected dust is estimated to weigh 1 mg/cm<sup>2</sup>. For the CRAF mission there seems to be no desire to expose the spacecraft to more than one or two monolayers of dust. Two monolayers would be 1/13th of the maximum load for the highest resolution sensor, 1/9th and 1/7th for the medium and low, respectively. Because of this, extensive testing was not done at extreme high loadings. The .01 cm<sup>2</sup> sensors are all tested at a  $6.6 \times 10^{-5}$  g load (equivalent to 6.6 monolayers of dust) because the calibration weight weighs that much. Similarly, the 1 cm<sup>2</sup> sensors all see a 2 mg calibration weight. Additionally, the .1 cm<sup>2</sup> and 1 cm<sup>2</sup> sensors were tested with loads of  $3 \times 10^{-4}$  g and  $3 \times 10^{-3}$  g, respectively, equivalent to 3 monolayers of dust. The sensor response to these loads has been to show the proper amount of frequency change, and a small amplitude change.

The mass resolution changes also, by the relation:

$$\text{loaded res} = (1 + n) \times \text{unloaded resolution}$$

where n = load expressed in  $m_0$ 's

For example, one monolayer of dust on a .01 cm<sup>2</sup> sensor ( $1 \times 10^{-3}$  g/cm<sup>2</sup> x .01 cm<sup>2</sup> =  $1 \times 10^{-5}$  g) represents 1/6 of an  $m_0$  (typical  $m_0$  of .01 cm<sup>2</sup> sensor is  $6 \times 10^{-5}$  g). Therefore the numerical value of resolution at a 20 second averaging time increases to  $(1 + 1/6) \times 5 \times 10^{-12}$ , which is  $5.83 \times 10^{-12}$  g. This is a modest loss of resolution from the nominal  $5.0 \times 10^{-12}$  g.

#### 4.1.4 Temperature Coefficient

Temperature coefficient is difficult to measure when near the optimum temperature, where the coefficient is zero. The difficulty comes from the need to be able to read very subtle changes in frequency while making major changes in temperature. There is always a small background drift in frequency due to evaporation of contaminants. Temperature changes can upset the rate of this evaporation, making it difficult to account for the "background". The best method found to determine coefficients is to manually make 2 to 4 degree jumps in temperature, randomly alternating increases and decreases, waiting long enough to try and re-establish background drift rates between changes. Data obtained by this method for sensors 923, with a .1 cm<sup>2</sup> stage, and 924, with a .01 cm<sup>2</sup> stage, are plotted together in Figure 17, with a least-squares fit line through all the data. The zero point is seen to be at 32.5 deg C and the slope of the line is:

$$- 1.21 \times 10^{-7} \text{ Hz/Hz-deg C /deg C}$$

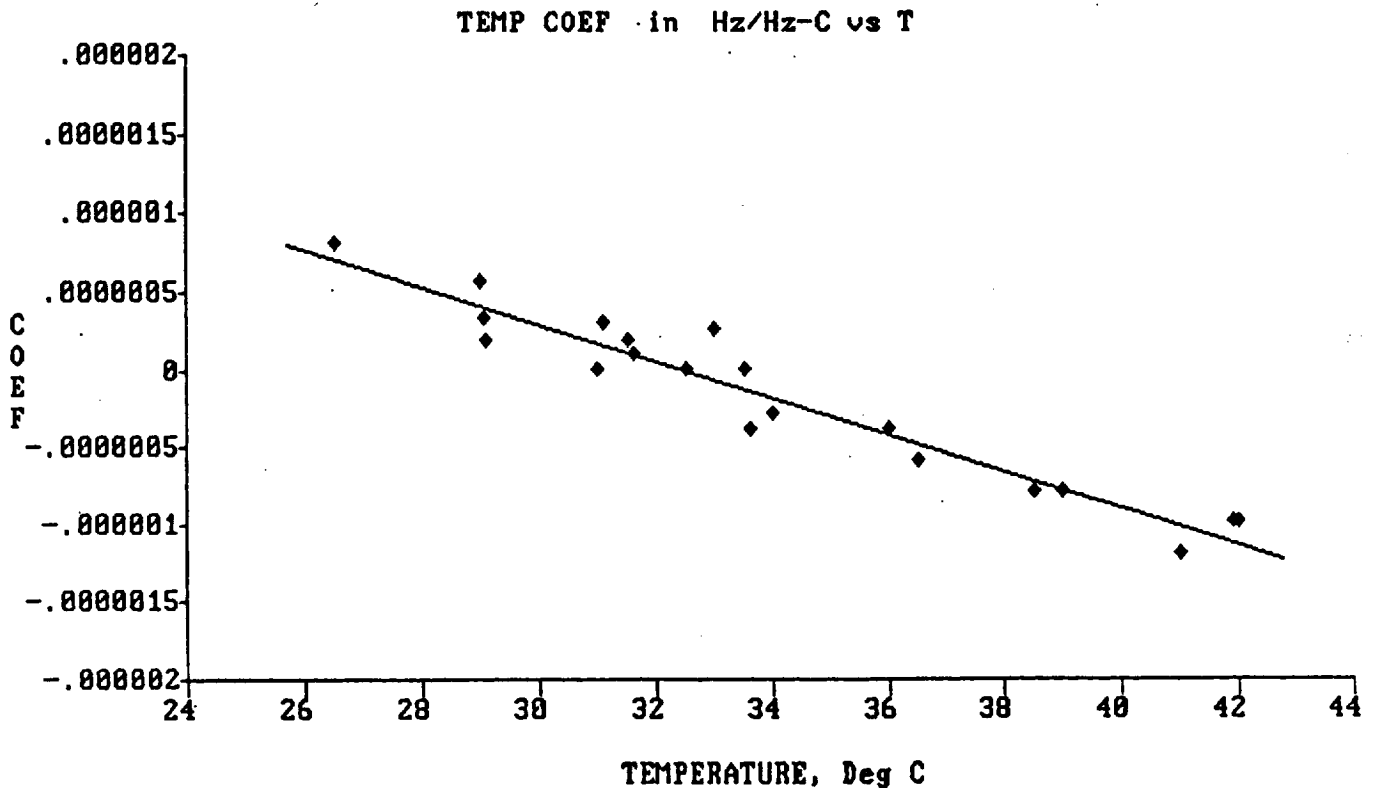


Figure 17. Temperature Coefficient of Frequency for Sensors with SiC Collection Stages

The sensors made with Be stages have a different temperature coefficient from ones with SiC stages. The slope of the line seems to be a bit less, which means less change in coefficient with temperature, but the line is offset by  $-9 \times 10^{-7}$  to  $-7.3 \times 10^{-6}$  hz/hz-deg C at 32.5 deg C. The offset repeats on different tests of the same element sensor with different mounting conditions, with different physical amplitude, and with different PD current. There are two possible explanations. First, the elements may not have been fully annealed after forming and stage attachment. A similar offset,  $-1.2 \times 10^{-5}$  @ 32.5° C was seen when a low temperature metallization was used and the element consequently saw no anneal at all. The larger element may require a slightly higher temperature or longer dwell to remove the offset. This removal of the offset occurred with the unannealed elements when they were later annealed. Unfortunately, the discovery of this offset in the final 1 cm<sup>2</sup> element was discovered too late to make more, and it cannot be re-annealed once the Be stage is attached. The issue can be quickly resolved whenever production is resumed. Another, less likely possibility is that the polyester bonding agent either changes its physical properties with temperature or distorts the Be stage with temperature. Figure 18 shows the temperature coefficient of 2 sensors with 1 cm<sup>2</sup> Be stages, using the same X axis as in Figure 17.

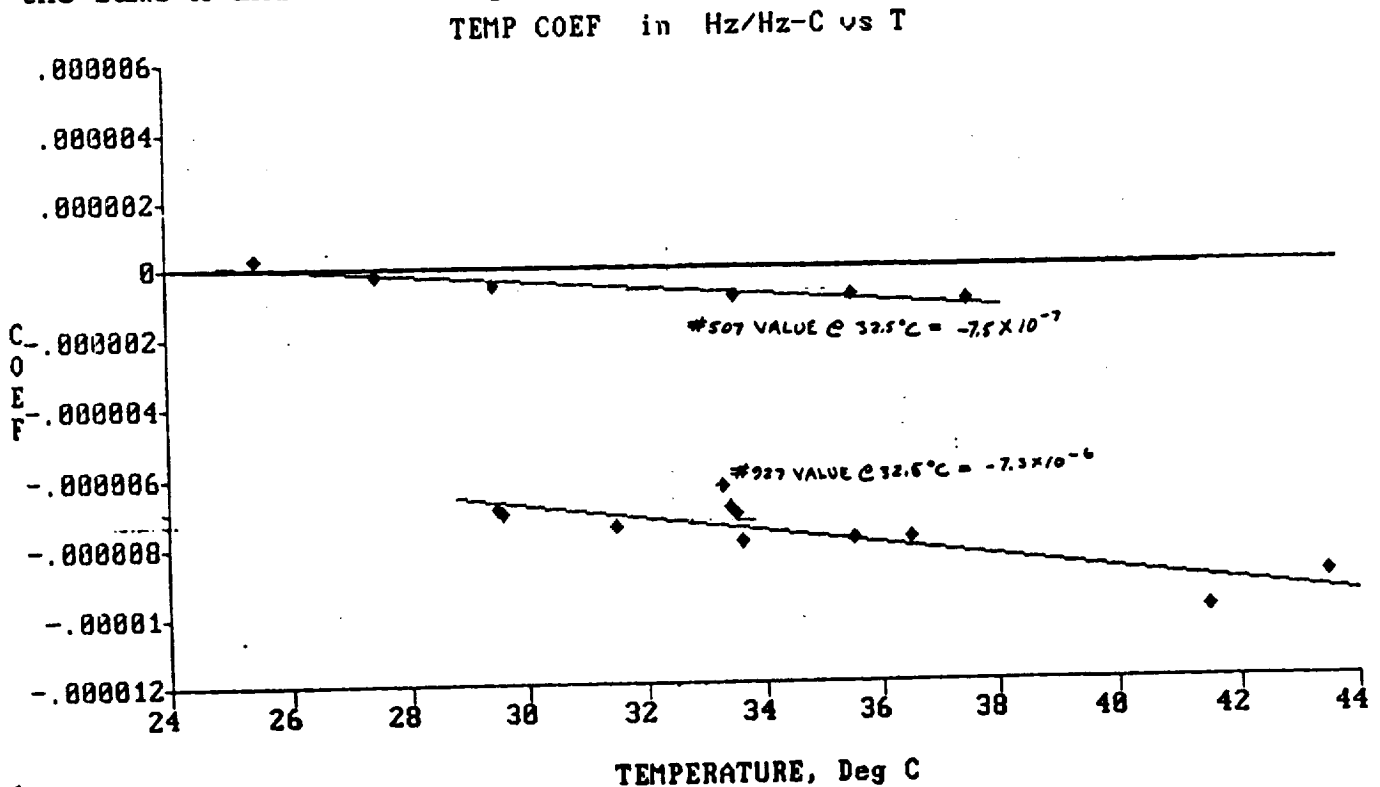


Figure 18. Temperature Coefficient of Frequency for Sensors with Be Collection Stages

For individual particle measurements, temperature coefficient can be neglected. For accumulation readings over the long term (days or weeks), temperature may unavoidably change several degrees. In this case, the temperature coefficient at a temperature midway between the starting and ending temperatures should be used to correct one frequency (not both). Then the mass difference can be calculated in the normal way. For example:

$$dhz = \{Tempcoef@[(T_2 - T_1)/2]\} \times F_1 \times (T_2 - T_1)$$

Add dhz to  $F_1$  before calculating mass change. This correction scheme requires that the sensor be at a uniform temperature and not have significant temperature gradients. Since this was always to be the case for CRAF, no attempt was made to study the effects of temperature gradients in the sensor.

#### 4.1.5 Environmental factors

This contract was entered into with the idea that the sensors should be suitable for any number of applications in space. One mission in particular, CRAF, was used to provide environmental data for the testing of the sensors.

##### 4.1.5.1 Vibration

The vibration environment during both launch and flight would seem to be a major concern for devices whose basic operating principle is harmonic vibration. The concerns are divided into two areas. The first is survival of the launch vibration environment. This environment has been defined for CRAF, using a shuttle launch and Centaur upper stage. Eight sensors, including at least one final form example of each size, were subjected to the random and sweep vibration environments specified in the proposal information package for the CRAF mission. The result was that all sensors passed. The tests were actually gentle compared to what the sensors can take. A special report was issued at the conclusion of the tests and can be found in Appendix I. In an attempt to get the sensors to at least respond to the vibration inputs, much higher levels of vibration were tried, and the frequency range was increased upward to include both the primary and secondary resonant frequencies. The sensors not only didn't break, they didn't even appear to start oscillating. The theory for this is that the Q of the sensors is sufficiently high that the input frequency has to very closely match the resonant frequency to start oscillation, and in a sweep, there are only a few dozen cycles of the proper frequency, not enough to start oscillation. In preliminary vibration tests at R&P, very careful tuning of an eccentric weight shaker table

running at constant frequency was needed to excite the sensors. Only at 6 to 8 g's would the tapered elements oscillate enough to hit the drive plates, and hitting the plates for many minutes caused no detectable damage.

The second area of concern is vibration of the spacecraft while the sensors are taking data. Discussions with CRAF staff led to the conclusion that there were no expected constant vibrations of the craft, although pointing corrections and indexing of samples or lenses on other equipment might cause some shocks.

It is one of the great advantages of a TEOM® type sensor that shocks, no matter what amplitude, cannot be confused with a particle in the data. A particle landing causes a permanent frequency shift, whereas a shock does not. The worst that a prolonged series of shocks could do would be to make it difficult to resolve individual particle events during the noise episode. The total mass of particles accumulated during the noise episode would still be available as soon as the shocks ceased. The permanent frequency change with accumulated mass guarantees this.

A continuous background vibration would cause some loss of resolution to the sensors. A mention was made of ".1 g or less" in the AO for CRAF, but it was not clear if this referred to shocks or continuous vibration. On the basis of this sketchy information a test was devised. A .1 cm<sup>2</sup> sensor was mounted on a spring suspended platform with a motor driven eccentric weight driver. The driver was powered and an accelerometer on the platform was monitored through a spectrum analyzer. At low speed the driver produced almost a white noise, flat topped between 360 and 430 hz at .1 g, and trailing off slowly at higher and lower frequencies. The resolution of the sensor degraded from  $5 \times 10^{-11}$  g to  $2 \times 10^{-10}$  g at 20 seconds averaging times, a significant but not overwhelming amount. Once the design of a particular spacecraft is fairly mature and background vibration levels can be estimated, simple testing will show whether some sort of damped or isolated mounting is needed for the sensors. At present no special mounting appears necessary.

#### 4.1.5.2 Electrical Noise

There are two concerns about electrical noise, that coming in and that going out. The sensor has 6 leads, exclusive of temperature sensing and/or control. Four are at a DC potential or ground, and hence are not potential sources of noise. Of the two remaining leads, one is a low impedance AC near sine wave current loop at the oscillating frequency, (100 to 300 hz) with a maximum AC current of about .1 ma rms and a maximum DC current of about .5 ma. Not much potential for

interference here. The other lead (drive) is a high impedance open end circuit isolated from the drive circuit through a step up transformer. The AC waveform here is also a near sinusoid at 100 to 300 hz and is at 15 to 150 volts rms. As it is open ended, there is no detectable current in this line. This line also seems to present no problem for noise radiation.

Noise pickup is avoided by use of the low impedance current loop for the motion sensor. The high impedance drive line is susceptible to rf noise pickup, but the noise can do no harm. It is grounded through the transformer at the amplifier end before it can get into any mischief there. At the sensor end the tapered element is a high Q tuned system which will not accept any energy which is not at its resonant frequency. It is assumed that the DC lines will be adequately bypassed by whoever packages the analog circuit.

## 4.2 Durability

The tapered element is admittedly a delicate item when out of its housing. The glass it is made of is in a family of glasses known for strength and chemical resistance. As with any glass mechanical part, the most critical area for stress is where the glass is attached to the metal of the rest of the structure. The ideal connection for any glass part is one where the glass and metal have matched coefficients of expansion, where any exposed glass has smooth rounded edges, and where there is no stress imposed by clamping forces on the glass. The Kovar-glass seals made for vacuum systems are a classic example of the ideal joint between glass and metal. By using a fused and annealed joint instead of a clamp, there are no residual stresses in the glass to propagate the minute surface cracks which are present in all glass. The design of the tapered element is also an ideal situation for glass in that the element is free standing, requiring no mechanical attachments other than the base and a looped soft wire for the drive. The element is at risk during manufacture and assembly, but once installed in the housing, is at no more risk than the countless glass to metal sealed insulators used in making hermetic IC packages for spaceflight. The most delicate part of the sensor is obviously the very small stage and its connection to the glass, but once again, there is a good expansion coefficient match and the joint can be annealed to prevent failure from residual stress. The silicon carbide single crystals and pure beryllium foil used to make the stages are two of the stiffest and strongest materials available. The connection has also proved to be very strong. In destructively testing the joint between the tapered element and SiC stages, it is the strong stage that breaks first, not the connection. The fact that the stages are very small is one of the things that helps. They have so little mass of their own that they cannot be induced to "beat themselves apart" any more than shaking a

feather can hurt it. The tapered element is free standing, so the only loads to be born by the stage are g loads and the static load of the accumulated dust. To test for static load carrying ability, the SiC stages have been loaded with the equivalent of a hundred times the CRAF mission load and the Be stage 20 times with no ill effects. The vibration test described in the previous sections confirmed there were no g load problems.

The durability of the housing as designed was also confirmed in the vibration tests run, but as mentioned previously, the configuration of the outside, and therefore the structural strength, of the housing will probably change in the accomodation phase between the instrument builder (for CRAF, a JPL appointed contractor) and the sensor builder (R&P).

#### 4.3 Manufacturing and Quality Control

In this section the qualitative and quantitative manufacturing specifications which yield durable and reliable high performance sensors are considered.

##### 4.3.1 Materials

This is a complete list of all materials used in the construction of all three sizes of sensors. Any product numbers or known applicable standards are shown as part of the description. Following the listing is a brief discussion of particular properties critical to the sensors and how to test these properties if no official standard exists.

Light Emitting Diode (LED): Texas Instruments TIL24, on JPL preferred parts list ZPP-2061-PPL, SCRNs SPEC 2073-3037, DWG ST 11732. This item is a fully qualified part, selected for "overall excellence, high usage history, and availability".

Photodarlington transistor (PD): Motorola MRD370, on JPL preferred parts list ZPP-2061-PPL, SCRNs SPEC ZPP-2073-8168. In listing this device JPL has derated the power spec to 125 mw. This application always runs at 15 mw or less, well within the derated limit.

Field plates, LED holder, PD holder, drive wire holder: copper clad PTFE printed circuit board material. Military grade FLGX, in 1/8 and 1/4 inch thickness.

Assembly hardware: All 2-56, 316 SS cap screws and washers.

Solder: 60-40 Electronic grade rosin core.

Connector and wires: Prototypes use ITT Cannon MDB1-9SH003-095479-0023. This is a good quality, gold contact miniature

connector with potted, PTFE insulated wires. It should not be used for the flight units because there is evidence that the plastic body deteriorates at high temperature in vacuum. JPL STD00009 should be helpful in selecting a connector once the location and orientation are agreed upon between the sensor builder (R&P) and instrument builder. Wire such as Belden 01 RK 83002 26 awg, 7 x #34 has performed well on all prototypes.

Housing body and mounting brackets: Items 0012HEAD, Housing body (1); 0016HEAD, base(1); and 0017HEAD, plate holder and backup plate (2 ea) make up the aluminum parts that support and locate the optics, drive plates and tapered element. These parts are designed for rigidity, not strength per se, so can be made from any grade of aluminum, or magnesium if lighter weight is desired. No finish which has any possibility of flaking or dusting should be applied. The prototypes had no applied finish.

Slit: The slit, 0018HEAD, which defines the LED's beam, is made of brass shim stock for ease of fabrication. A stainless steel piece would be equally functional and probably be a better material for long term (years) vacuum exposure. Once again no applied finish was used. No matter what material the slit is made of, a brushed or rough finish is better than a specular one.

Temperature sensors: For the prototypes, two thermistors, YSI P/N 427, were clamped to the housing body with two brass clips, 0019HEAD. The thermistors and clips were selected for compatibility with the temperature controller, YSI 72, used in the vacuum chamber. The flight unit should probably use at least one RTD, which has better vacuum compatibility and long term stability than a thermistor, but that is the instrument packager's prerogative.

Tapered elements (and the blanks as they appear before pulling): are dimensioned by R&P Dwg. # 0032HEAD. There are nine materials used to make tapered elements.

- 1) All elements start out with a commercial 3/8 inch Kovar to glass vacuum system transition fitting. These are commercial items of high quality made in quantity from specific grades of Kovar tubing and glass tubing.

- 2) All elements utilize a 3 inch length of "LC" (low coefficient) glass tubing, a proprietary glass made by Corning Glass Works only for R&P. This length of glass is fused to the length of Kovar tubing by cutting the glass attached to the commercial seal to 1/4" long and then fusing the "LC" glass tube to the commercial glass.

- 3) All elements get a coating of platinum using Hanovia

#05-X. This coating goes on the large end near the Kovar base where the solder joint for the drive wire will be.

4) All elements get a full coat of Engelhard Liquid Bright Gold #4813 over the entire glass part of the element except for a small insulating ring left clear near the Kovar.

5) All elements have a small shard of glass of the same type as the glass used for the commercial Kovar tube base melted onto the small end of the element.

6) .01 and .1 cm<sup>2</sup> elements use single crystal silicon carbide for the stages. Two types of material are suitable. The best all around material comes from semiconductor work going on at NASA Lewis, kindly provided by Tony Powell, who has a large stock of suitable material in his sample archives. This is "Beta" SiC, grown on a silicon substrate, which is etched away before use. It is very easy to cleave into squares and is very flat and uniform. There is also available some "Alpha" SiC, from sources such as American Matrix. The Alpha material seems stronger, but has different cleavage planes and is much harder to cut into a regular shape. Not having been grown on a substrate, the Alpha often has small crystals growing on or out of the surface. Thickness can vary substantially, as well. However, American provided some "almost good enough" samples and is improving their capabilities. They should be contacted for their latest status when flight equipment is actually contracted. Norton Co. and R.F.Davis at North Carolina State are also active in the growing of SiC flat stock, and also should be contacted for updates if the flight equipment is contracted in 1989 or later.

7) The 1 cm<sup>2</sup> collection stage is made of .5 mil pure beryllium foil from Brush Wellman. .5 mil is the thinnest that can be supplied with assurances of flatness and nonporosity. The grade specification is PF60. All prototype stages were made from material rolled to .0005", and came from lot 3244B. About 10 cm<sup>2</sup> remains from the original lot, as well as some thicker material, .002" thk, from the same lot. The thicker material could be etched leaving ribs if larger or stronger stages were desired. Any stage over about .15 cm<sup>2</sup> in area should be made from the Be, since the SiC is hard to handle and cut in the larger sizes.

8) When a 1 cm<sup>2</sup> stage is used, the glass shard (item 5) is first melted onto a small piece of Kovar foil. About 2 mm<sup>2</sup> are used, then etched away once the glass is fused to the tapered element. The foil used is 2 mils thick and about 2 mm<sup>2</sup> is used for each 1 cm<sup>2</sup> tapered element. A minimum order of several square feet was obtained and is carefully packed in corrosion preventive foil for future use.

9) When a 1 cm<sup>2</sup> stage is used, a small amount of adhesive is used between the flat formed against the Kovar and the bottom of the Be stage itself. The adhesive used is Bostik 7064, a high heat resistant polyester adhesive. It is mixed with a curing agent, Boscodur #1, which has a polyisocyanate base. The adhesive was selected for its high heat resistance, 155 to 180 deg C, and because it is a laminating adhesive which can be completely dried of any solvent before closing the joint at 160 deg C.

#### Notes on materials:

LED: It has been remarked by a researcher at EOS that the aim of the LED's beam can be off by as much as 5 degrees from its physical axis. The present mounting system allows for this. A "more precise" mounting and aiming system for the LED would be no improvement if it does not allow for this internal variation in aiming. A return wire from the sensor can be eliminated if a resistor is installed at the LED, but this would eliminate the possibility of stringing the LED's in series to save power.

PD: This device has a broad acceptance angle, which is good in that it does not have to be aimed very carefully, but bad in that it will pick up stray light and should be well shielded from stray light. It also has a phase delay which varies with temperature, which can be minimized by keeping at least .2 ma of DC current flowing in it. This is done by allowing some light to get to it from the LED which is not blocked by the tapered element. Since the phase variation with temperature is not a documented feature, a few samples of any new lot should be checked for this parameter using a modulated LED with a DC bias in a temperature controlled setting.

Field plates, assembly hardware, solder, housing body and brackets: All these items should be cleaned and deburred carefully before and after assembly. Tapped holes should extend through the housing or intersect other holes to help clean out cutting oil and avoid trapping gas. If any anti-corrosion coatings are required by NASA specifications, they absolutely cannot dust or flake in any manner. Bare surfaces are to be preferred. The body interior may have to be treated for good emmissivity, depending on what the thermal control people want. If so, once again there must be no chance of dusting or flaking of the paint or anodize used. No problems were encountered using bare metal surfaces in testing the prototypes.

Connector: If, as has been suggested, the analog board ends up mounted right next to the sensor to help keep it warm, the connector may be omitted and the wiring run direct from the sensor wiring points to the board.

Slit: The slit defines a beam, but because of the divergence of the light the beam is actually quite wide by the time it gets to the tapered element. Because of this, only one edge really does all the work of defining the "beam". In fact, a single edge "blocker" was used on some sensors with good success. The present function of the second edge of the slit is to limit the extra unmodulated light going to the photodarlington, and it is this function rather than defining a certain "size" beam that determines the slit width.

Notes on materials for tapered elements:

1) Kovar-glass seal: Vendor quality control has been good, but dimensions and roundness of the Kovar should be checked, as well as a visual inspection for a uniform gray color and lack of cracks or dirt at the glass-Kovar interface.

2) "LC" glass: At present, and for the foreseeable future, this glass is made in lots of a few kilos and formed into tubing on a semi-manual machine. The tubing machine is more subject to dirt and streaks than normal production line machinery, which processes tons per hour and flushes dirt out by dint of sheer volume. A bubble or dirt speck in the part of the blank which is to be drawn down into the tapered element would not be good, but this is a small and well defined area of the blank. Careful visual inspection under a low magnification ring light is all that is needed to assure that the particular inch of tubing which will be drawn has no defects. Major defects are of course cut out by Corning, and minor closed bubbles or encapsulated dirt pose no hazard in the discarded part of the blank or the large part of the finished tapered element. "LC" glass and the commercial glass which comes attached to the Kovar have different indices of refraction which results in a line of demarcation at the fused joint near the base of the tapered element. This line is not a defect or weak point, and should be used to make sure that the glass on the Kovar was cut short enough so that none of it ends up in the small diameter part of the tapered element.

3) and 4) Platinum and gold coatings: All solvents used to clean brushes or thin the gold for application on the thin tip should be certified reagent grade. Sable brushes are recommended to get smooth coatings, and the elements should be inspected for skips or drips both before and after firing. The finished coating should be examined under at least 50x and checked for peeling or skips caused by contamination. A semi-transparent coating is still thick enough to be sufficiently conductive, and is preferred to a totally opaque coating, which is harder to inspect and has to be examined especially carefully for small peeling spots.

5) and 6) Silicon carbide and glass shard: After cutting, the stages have to be carefully examined in cross lighting for cracks induced in the etching or cleaving operations. Any cracked stage should be rejected or re-cut for the next smaller size. After fusing, the "footprint" of the glass on the SiC should be at least 25% of the diameter of the glass shard (which will have formed into a ball). The end of the tapered element should not have a sharp bend in it near the stage, although a gentle bend is no defect. The entire circumference of the end of the tapered element should also be completely immersed in the glass ball and not be visibly ragged or cracked in any way. The stage should be at a right angle to the axis of the tapered element, and should be within 1 element diameter of being centered.

7) Beryllium: The Be foil must be handled carefully to avoid kinking or curling it. All cutting should be chemical, as it fractures when sheared. Removal of masks should also be chemical to avoid curling the flat foil.

8) Kovar foil: Kovar can be magnetized and should be kept away from magnetized tools to avoid problems positioning it with tweezers used on the fusing hotplate.

9) Adhesive: Reagent grade solvent should be used for dilution to avoid contamination.

#### 4.3.2 Processes

Many standard processes, such as machining and soldering, are used to make these sensors. There are existing quality standards for these processes, which need not be discussed here. Other processes, such as joining glass tubes and firing metallic coatings, are commercial processes which are widely used. They need only be discussed in terms of any special requirements needed to assure high quality and reliability. The commercial process is not changed, just monitored more closely to assure that it works as intended. There is a third set of processes, actually only two, which are unique: joining of the stages to the tapered elements and the final alignment and adjustments of the sensors. The quality assurance aspects of these two operations will be discussed in detail.

The manufacturing and quality control processes used to build up a .1 or .01 cm<sup>2</sup> SiC stage sensor will be described chronologically starting with the making of the tapered element. Standard processes will be mentioned only by name. Commercial processes will be discussed in terms of the extra monitoring, control, and/or inspections needed. The two unique processes will be fully described and discussed. After this description,

the changes needed to make a 1 cm<sup>2</sup> Be stage sensor will be noted.

The first operation is to cut the glass on a Kovar-glass seal to 1/4" long. This is done using a low speed, fine grit diamond blade leaving a smooth, flat surface. This is done in batches and the pieces are then washed, dried, and packed so they will not scratch one another. Lengths of "LC" glass are then inspected and scratch cut to 3" lengths by a skilled glassblower. He then fuses the glass end of the Kovar-glass seal to the "LC" glass tube, making a uniform blended transition and carefully keeping the "LC" glass on axis with the Kovar tube. The finished blank is once again washed and dried and the uniformity of wall thickness is checked. The blank is installed in the computer operated puller for the first operation. The thick wall side of the tube is always installed toward the top to promote uniformity from pull to pull. The first puller operation is to heat the glass and, by means of a vacuum, shrink the section which will form the thin part of the tapered element onto a mandrel. This increases the wall thickness and assures that all elements are pulled with the same starting ID. The mandrel and blank are allowed to cool and the mandrel is removed. The blank is now inspected to make sure the collapse was uniform and the ID is now circular. The next puller step is to once again heat the glass and this time pull it slightly and then apply a vacuum again. The heating is such that the glass is softer in two opposite quadrants. The vacuum pulls the glass into an elliptical shape. The glass is allowed to cool. The ellipse is inspected for symmetry and ratio, and the length of pull is checked. The last puller operation is now started, and the glass is heated, pulled, reheated, and pulled one final time to complete the shape of the element. The length of the final pull is predictive of the  $m_0$  of the element. The key technology of the puller is that it senses the viscosity of the glass and can use either viscosity of the glass or elapsed time to decide when to move to the next step.

Once the glass is shaped, the next step is to platinize the base. This step also serves to anneal the Kovar to glass joint, the glass to glass joint, and the shaped "LC" glass. The platinizing solution is painted on like shellac, air dried, and then fired using a programmable controller on a lab furnace. In commercial work a tunnel kiln is used with the work moved through the various temperature sections continuously. The programmable controller duplicates the temperature history of the commercial kiln. The coating requires oxygen, first to burn out the organics in the coating and then to oxidize the small amount of base metal in the coating which bonds it to the glass. This oxygen also oxidizes the Kovar somewhat, so the elements must be handled carefully to avoid dropping any oxide into the small end. The elements are carefully inspected for internal dirt before

proceeding to the next step. Trapped dirt can usually be removed by a sharp rap on a tabletop. If not, the element is rejected.

The gold coating is now applied. It is applied the same as the platinum on the base end, and is thinned for better flow out before being applied to the thin end. The shellac-like coating has a tendency to bead up and leave bare spots on the thin end if not thinned and applied carefully and uniformly. It is easy to inspect when dry, however, because of its fairly strong tint which shows bare spots or heavy spots clearly. If any bad spots are found, it is an easy matter to remove the coating with a drop of solvent and recoat before firing. Careful visual inspection is required but wholly sufficient to prevent any defects. The firing is conducted the same as for the platinum. The gold over platinum coating on the base combines the tight and alloying resistant properties of the platinum coating with the easy solderability of the gold coating for the area where the drive wire must be attached.

The drive wire is now soldered on. A single strand of fine tinned copper wire is wound around the base of the tapered element in the middle of the platinized area. It is then soldered at four places around the circumference, including the point where the ends spring away from the glass. The soldering iron tip should be drawn along the wire when leaving each joint to avoid leaving any roughness or loose solder bits. A good flux remover solvent and brush are then used to remove all traces of the rosin flux.

The tapered element is now ready for cutting to length. This operation determines the operating frequency and gives approximate values for the final  $K_0$  and  $m_0$ . The tapered element is mounted in a fixture where a DC field is supplied and a drive voltage can be applied to the drive wire. The drive is supplied by an audio oscillator which is tuned until the tapered element is oscillating at maximum amplitude. The tapered element is cut a little at a time by crushing the end with fine tweezers. The oscillator is retuned each time and once the frequency is over about 200 hz, a small weight is attached to the end of the tapered element with a tiny bit of grease. The oscillator is once again retuned, and by knowing the frequencies with and without the weight and the mass of the test weight,  $K_0$  and  $m_0$  can be calculated. Since the mass of the stage to be attached is also known, the final operating frequency and  $m_0$  can also be predicted.  $K_0$  will change very little after stage attachment. The cutting and application of test weight procedure continues until the predicted operating frequency is over 200 hz. At this point if the predicted  $m_0$  is too high or low the element is rejected. Rejects at this point might result if there were an abnormal variation in the raw stock wall thickness at precisely the cross section which was drawn down into the fine tip of the

element. One of the clippings from the last few trimmings is also examined under a microscope and the major diameter, minor diameter, and wall thickness are measured and recorded, as well as any asymmetry. If the clippings are lost, the end of the element itself can be examined, although this exposes the element to more handling which is not desirable at this unprotected stage. Before the element is removed from the fixture, it is rotated 90 degrees and the cross frequency is checked. This is a measure of ellipticity.

Now the element is ready for stage attachment. A small piece of the glass which comes attached to the Kovar is crushed and under a microscope a shard is selected. The shard should be a chunky piece, not a sliver or flake, and have a maximum diameter about 1.3x the major diameter of the tapered element to be used. The stage is now cut by lining up the line of cut over the etched line on a reticle and pushing the crystal into the depression with the sharpened end of a jeweler's screwdriver. The crystals break quite cleanly along natural cleavage lines which allow perfect squares or rectangles to be made. Once the crystal is inspected for stray cracks, it is ready to bond to the tapered element. The tapered element is affixed in a holder which has micrometer adjustment in the X,Y, and Z directions, as well as the ability to back off 2 or 3 inches in the Z direction without losing the previous coordinates. The holder positions the tapered element over a heated block of alloy titanium. The stage is placed on the heated block and the glass shard is placed on the stage. The tip of the element is used to nudge the shard to the exact center of the stage. The tapered element is now lined up so that the tip of the element is poised a few thousandths of an inch over the glass shard. This is all done under a stereo microscope. The element is backed off, and the heated block is brought to a high temperature by a programmable controller. The glass on the stage melts and forms itself into a ball. The heater is allowed to cool a little, and the end of the element is brought once again right over the ball. Any final centering is now done, the element once again backed off and allowed to cool, and then the element tip is plunged all at once into the ball, encasing the end of the element and flattening the ball against the stage. The element is now lifted a few mils, taking the stage with it. The end of the element usually gets bent a little in this operation, and the stage is now hooked under a "T" slot and the element pulled enough to straighten it. The stage is dropped a little, taken out of the slot, and dropped to touch the hot plate once more, establishing the plane of the stage at a good right angle to the axis of the element. The stage is now lifted about 100 mils over the heated block and the heater is turned off and allowed to cool slowly. Once cooled, the tapered element is moved to another fixture which allows rotation and the stage attachment point is examined carefully for centering, uniformity, complete fusion of the end of the element,

and a substantial "footprint" on the transparent SiC. If any defects are found, the tip of the element including the stage is snipped off and a new stage is prepared. This can be done several times before the tapered element gets so short that the operating frequency goes too high. With some practice, 90% of the stage attachments will be good on the first try.

The completed tapered element with stage is now ready for attachment of a base. The Kovar tube is cleaned and its diameter measured to within .0001". An aluminum base is prepared with a hole about a mil less in diameter than the Kovar OD. The tapered element length is measured and spacers are assembled in a fixture on a hotplate. The spacers allow the Kovar tube to drop through the aluminum the proper amount so that the stage will be at the right height in the housing. This "custom fit" allows for slight variations in finished length of the tapered elements with stages, and allows all three sizes of sensors to be installed in the same housing. The base is heated to 300 to 400 deg C and the Kovar tube dropped in; then the whole assembly is allowed to cool. This is all pretty much a standard shrink fit as any machine shop would do it, with one feature which makes it unique. The Kovar has a very low coefficient of expansion so it does not have to be kept cool. In addition, the joint can be taken apart or readjusted by just reheating it.

The element is now taken back to the calibration fixture to get the final calibration, determination of  $K_0$  and  $m_0$ , and determination of the running and cross frequencies. For best results, the calibration weight should be cleaned and the attachment grease applied only to the stage.

The tapered element can now be set aside while the housing is wired and assembled. The only quality related issue not covered by standard practice in assembly and soldering is that all tools, especially Allen wrenches, should be cleaned before use so as not to leave grease or dirt in the screw sockets.

The tapered element can now be installed in the housing and its drive wire soldered to the drive wire holder. The element is centered by eye in the housing and the base tightened down. The optics and slit are assembled and aligned roughly by eye to be centered in the housing. The sensor is now powered up. An oscilloscope is used to monitor the PD receiver output signal and a milliammeter is put in series with the PD. Most of the time this alignment is good enough that the sensor oscillates right off, and only minor adjustments are needed. The amplitude of oscillation is increased until the normally sinusoidal output of the PD clips. The slit is adjusted until the clipping is equal on plus and minus swings. The drive is decreased to the normal running level, then the LED is adjusted to give the

maximum PD signal, and lastly the PD is adjusted for maximum signal. If the LED or PD hit the end stops of their limited travel, the slit is moved and the process repeated. If the DC bias of the PD is below .2 ma after adjustment, the slit can be opened another mil or two and the process repeated. If the tapered element does not oscillate after rough alignment, the calibration oscillator can be used to provide drive, and the optics can be adjusted until the PD picks up the oscillation. This was the method commonly used with the older housings and hand made tapered elements. The new housings and machine made elements are uniform enough so that they usually run right away.

The sensors should now be cleaned in an ultrasonic cleaner filled with Freon TF, and baked at 100 deg C for at least one hour in a vacuum oven. Ideally, the sensor is then taken still warm and installed in a heated sleeve and put in a clean vacuum system where drift and temperature coefficient can be determined. The sensor should be kept in a clean oil free vacuum system or at least in a clean plastic zip loc bag when not in use.

1 cm<sup>2</sup> sensors: Everything is the same up to the cutting of the SiC, which is replaced by punching out a small disc of Kovar and hammering it flat. The Kovar is used in place of the SiC. One difference is that the glass shard wets the Kovar when it melts, making a "fried egg" of glass on the Kovar, rather than a ball. Another difference is that the end of the element, being much larger, doesn't usually bend and need straightening. If the Kovar has been accidentally magnetized during preparation, it will "dance" off the heated block due to the block heater's AC magnetic field. Waiting to position the Kovar and glass shard until the block is hotter than the Curie point of Kovar is the solution. By the time the Kovar joining is over, the thin foil (where it was not protected by the glass) is usually quite corroded and flaky. It can usually be popped off the end of the element leaving a very flat black surface on the glass. If it doesn't pop off easily, it will come off when the end is etched. A 1:1:1 solution of sulfuric acid, nitric acid, and water is used to remove any remaining Kovar and most of the oxide. Some oxide is dissolved in the glass, and the result is a very flat, very black surface which is ideal in shape and texture for bonding. The acid can remove some of the gold, so it is best not to dip any more than the last 1/16 inch of the tip in the acid. The tip should be rinsed well and set aside while the Be stage is prepared.

The Be stage is cut by chemical blanking, a common way to make small quantities of thin metal parts. This is especially true of beryllium, which is very difficult to machine mechanically because of its great strength and stiffness. The beryllium stock is masked completely on the back with black vinyl

tape. Two circles are cut from two more pieces of tape. One circle, exactly  $1 \text{ cm}^2$  in area, is rubbed down smoothly on the front side of the Be foil. The other circle is cut somewhat larger; it is discarded and the tape it was cut from is used to mask the rest of the face of the Be foil, leaving only a thin ring exposed all around the  $1 \text{ cm}^2$  circle. A drop or two of ferric chloride are placed on the ring with a toothpick. This etchant will immediately wet and attack the Be yet bead up and retreat from the vinyl. After a few minutes the whole assembly of tape and foil are rinsed and dried. If any metal is seen in the ring, the etchant is applied for another minute. Once the ring is clear, the assembly of foil and tape are covered with a coating of any commercial solvent type paint stripper, which will soften the tape and dissolve the adhesive. The Be foil stock and circle are then retrieved and rinsed in mineral spirits and acetone. The extra foil is returned to stock and the circular stage is ready for attachment to the tapered element.

The stage can be attached with any vacuum compatible epoxy, polyimide, or polyester. A polyester laminating adhesive was used because it lends itself nicely to the fixtures already available for holding the tapered element and attaching stages. The adhesive is mixed and thinned and just enough to cover the diameter of the glass "fried egg" is placed on the tip of the element and on the stage. Both are dried using the heated block, and then the stage is centered and attached in much the same way as the SiC stage, only at much lower temperature. The actual sequence is to first complete the drying with the stage and tip of the tapered element near but not touching, then raise the temperature and tack the stage on by touching it. Next lift the stage clear while the heated block is brought to the curing temperature, and then bring the stage back down to touch the block and cure the joint.

#### 4.4 Drive Electronics

The analog circuit which powers the sensor and conditions the frequency output is not markedly different from the proven circuit which R&P uses in its commercial products. Most of the modifications were directed toward tuning the feedback circuit to be more appropriate to the very small, high Q tapered elements used here. The commercial elements are much larger and have lower Q because they always run in air.

One major change is the removal of a closed loop physical amplitude control. This was done for several reasons. First, there is always a little hunting or instability in any closed loop control, and it was felt that higher ultimate resolution (lower noise) would result from using a fixed drive voltage (open loop control) rather than trying to maintain a fixed amplitude

(through a closed loop feedback). Another reason was that it was thought useful to make the sensor read only frequency and ignore amplitude. This has the benefit of avoiding any change in frequency as a result of the LED or PD output changing due to temperature change or aging. An increase or decrease in electrical output due to temperature or aging would be interpreted by a closed loop system as a change in physical amplitude, and the circuit would make a real change in physical amplitude in trying to keep the electrical signal at the same level. Since there is a small change in frequency when amplitude changes, this type of interaction could produce a "temperature coefficient of frequency" which had nothing to do with the physical properties of the tapered element.

#### 4.4.1 Schematic and Description

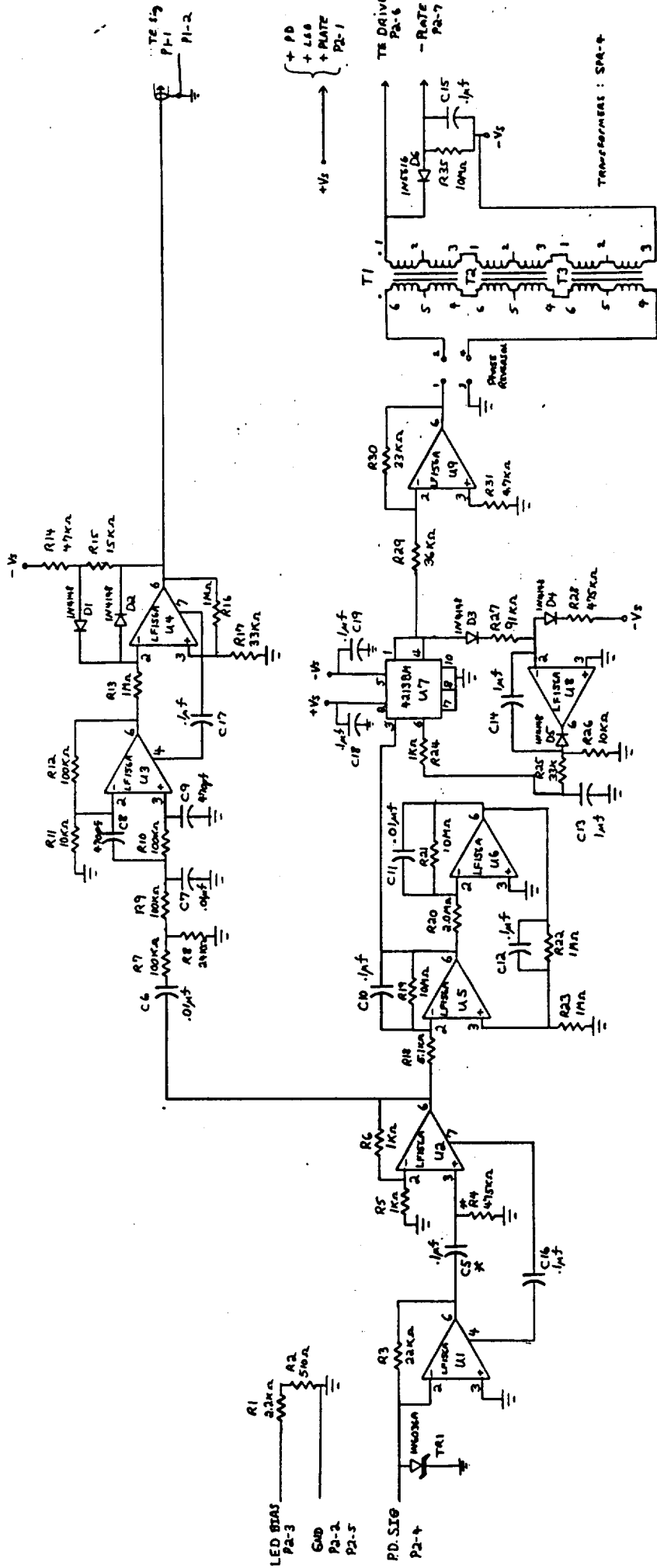
Figure 19 is the schematic of the analog circuit. It is composed of eight operational amplifiers and one special purpose IC, a multiplier. They are numbered in the order in which the signal travels through the circuit, so they will be described in numerical order along with any significant adjacent passive component circuitry.

U1 presents a virtual ground to the photodarlington and translates the current loop signal from the PD into a voltage signal. The extra diode on the input to U1 is a part of the ground test equipment and protects U1 from arcing if someone forgets to reduce drive voltage when going from operation in air to operation in vacuum during testing. Above U1 on the diagram is the dropping resistor for the LED, shown as two resistors so that one can be replaced with a potentiometer for experiments at which point the second one becomes a current limiter. For flight a single resistor would suffice. The LED's can also be run in series by tapping into the LED grounding lead here. By using a zener diode across each LED, one LED burning out would not disable all LED's in the series loop.

U2 is an isolator and amplifier stage. R4 and C5 act to correct the drive phase to exactly 90 degrees, compensating for any lag in the photodarlington. The gain resistor R6 is changed for each different size tapered element used.

U3 reamplifies the signal branch headed toward the counter after it passes through a low pass filter.

U4, in conjunction with diodes D1 and D2, forms a squaring circuit with hysteresis, transforming the sinusoid signal from the PD into a fast rise square wave suitable for counting. The hysteresis avoids multiple triggers if there happens to be noise



DATE	RUPPRECHT + PATASHNICK CO
8/25/67	
	TE FEED BACK AMPLIFIER
	FLIGHT VERSION
	FVAMP-01
	Page 1 of 1

Notes:  
\* Low TC. C5 AT LEAST 100ppm/°C  
R4 AT LEAST 25ppm/°C  
COMM PART NOS (1) ALL RESISTORS: MCGON... FS  
(2) OP-AMPS JMB3FD/11405 SEC (PMI)  
JPL PREF PART NOS (3) DIODES JAN IN... (TXU)  
NOT ON JPL LIST (4) MULTIPLIER 4E13W/M/RESE  
(5) TRANSFORMER SPA

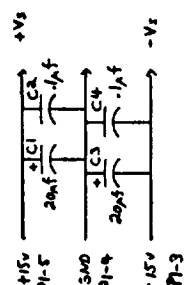
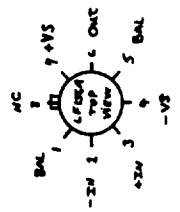
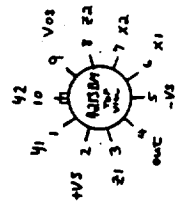


Figure 19. Schematic of Analog Circuit

on the sinusoid as it crosses 0.

U5 and U6 form a DC compensated integrator, providing the 90 degree phase lag needed to provide optimum drive. The time constants here are carefully tuned to damp transients quickly and keep the self oscillation inherent in this type of circuit below 100 hz.

U7 is a multiplier, configured here to act as an automatic level control. The integrator gain changes with frequency, and the PD and LED output vary with age and temperature. All these effects are ignored by having the multiplier hold the drive AC voltage constant using the -15 v supply as a reference.

U8 compares the rectified multiplier output with the -15 v supply and provides a properly damped correction voltage to the multiplier control input.

U9 takes the constant voltage multiplier output and drives the transformer(s). U9 may not be necessary for the small stage sensors, but does make it easier to adjust drive voltage by picking a value for R30, rather than resetting the multiplier output. It also isolates the multiplier feedback loop from the transformer inductance, which may be important.

The output transformer is shown as three discrete units. This was done so that only a single part number would be needed, and the number of transformers could be varied for the different size sensors which need different drive voltages. The 1 cm<sup>2</sup> sensor uses all three, the .1 cm<sup>2</sup> two, and the .01 cm<sup>2</sup> one. The particular turns ratio and impedences required here are not available in an off the shelf JPL flight approved version, but this is the usual case for inductors. There are several vendors who custom manufacture this type of transformer to flight approved specifications.

The rectifier circuit on the transformer output provides a high voltage DC for one field plate without increasing the number of supply voltages needed for the instrument. It also allows use of a smaller transformer than would otherwise be needed. A careful weight/parts count/power analysis performed when packaging this circuit for flight might show that a second diode and capacitor should be added so that the second field plate could be at a voltage higher than +15. The weight of the extra parts and extra lead to the sensor would have to be balanced against the possible reduced weight of the transformer.

#### 4.4.2 Parts List, Including Weights

All parts on this list except the multiplier and transformer are taken directly from the JPL preferred parts list. By the time the contract for the flight circuit is let, something similar to the multiplier may be on the list. If not, a waiver should be sought because it is available to very tight military specifications and would need to be replaced by many discrete parts if the circuit were redesigned around approved parts only.

The transformer is discussed above and it should pose no problem to get a flight approved version made.

DESCRIPTION / PN	QTY	WEIGHT EA,g
Operational Amplifiers, PMI JM38510/11405BGA	8	.9
Multiplier, Burr Brown 4213WM/883B	1	.9
Diodes, Unitrode JANTXV 1N5616	1	.3
Unitrode JANTXV 1N4148-1	5	.2
Capacitors, CRC J11B104JSA .1 @ 50	2	3.4
CRC J11B103JSA .01 @ 50	2	1.6
Sprague M39006/02-1232 20 @ 25	2	4.1
CRC P12B105JSW 1 @ 50	2	3.9
CRC P12E104KSW .1 @ 400	1	4.8
Kemet M39014/02-1350 .1 @ 100	6	.5
AVX CKR05BX471KR 470 pf	2	.4
Resistors, RNC 55 J xxx FS 1/4 w mf to 1M		
RLR 07 C xxx FS 1/4 w mf 2M		
RCR 07 G xxx JS 1/4 w cc 10 M	30	.2
Transformers Triad-Ultrad SPR4	1-3	7.1

#### 4.4.3 Power Consumption

The main power saving emphasis was on those elements which reside in the sensor. The drive and field plate connections draw essentially zero current, so the optics are the power items in the sensor. Since the sensor was to be the prime emphasis in this contract, and the analog board was modified only as needed in support of sensor work, it got less emphasis. Where choices had to be made, the low power alternative was always picked, but there is the possibility that if a concerted effort were made to find and test low power, flight approved operational amplifiers, the total power for the sensor-analog circuit combination could be reduced substantially. The op amps used typically draw 3 to 4 ma at +/- 15 v. Op amps are available which draw .3 to .6 ma which may be suitable for some or all of the functions needed.

With the components listed above, the total power for a sensor and circuit board is just under 1 watt, with slight variations depending on the size of sensor, operating frequency and optics alignment. An approximate breakdown is as follows:

ITEM	POWER, mw	NOTES
LED	7.5	same for 2 or 3 if arranged in series
PD	4.5	
U1	86	current to voltage converter
U2	196	isolation/amplifier/phase correction
U3,U4	189	lowpass/zero cross
U5,U6	182	integrator
U7,U8	208	multiplier/ ALC
U9	118	Drive amplifier
TOTAL	991 mw	

#### 4.5 Flight-like Housing, Including Weight

The housing has been discussed in detail in section 4.3, but to keep all the weight and power information close together in the report the weight breakdown is presented here.

Housing without TE or trim		34.5 g	
Aluminum base		9.0 g	
Kovar tube base	approx.	3 g	(varies)
Glass part of TE		4 g	
LED & PD holders, field plates		4 g	
Aluminum plate holders		1.9 g	
Screws	approx.	.2 g	ea
Sensor with all wiring and hardware, 2 temp sensors, no sleeve:	approx.	63 g	

Once decisions have been made regarding the best way to mount the sensors and viewlimiters in the instrument, more effort could be made to shave weight off the sensor. Four or five grams could be saved on the aluminum TE base, 5 or 10 grams on the basic housing, and another gram or two by eliminating some screws. Elimination of the connector and its mounting screws would also be a possibility if a set of pigtailed for hard wiring to the board were provided.

#### 5. Conclusions

- All performance and durability goals have been met for all three basic sizes of sensors.
- Particles in a wide range of sizes have been caught and weighed with resolution going into the  $10^{-13}$  g range for long averaging times.
- The critical pieces of high quality manufacturing equipment have been developed and put in place.
- A quality control program has been developed.
- Several different research groups are currently interested in purchasing and using these sensors in the space program.
- A portable self-contained instrument is available for demonstration purposes.

## 6. Brief Look at Remaining Work before Flight

### 6.1 Sticky Material Stability and Efficiency

Investigation of the sticky material used to collect dust was not made part of this particular contract since it was a common concern among several CRAF dust analysis experiments. The Dow Corning high vacuum (silicone) grease used in the dust experiments conducted under this contract was satisfactory as used, and indeed has been the standard against which all other candidate materials studied over the years have been measured. The questions which have been raised concern proof of long term stability and collection efficiency, which were not explicitly addressed in the "thrower" experiments. Efficiency is addressed in a recent major study by Ben Clark and Patrick Thompson at Martin Marietta. Long term stability has been addressed in the past by Ben Clark and will be taken up in the particular case of long term stability on silicon carbide and beryllium in a one-year study to start in 1988.

### 6.2 Coordination of Instrument Design with Sensor Properties, Especially Temperature

The basic design work has been done for the viewlimiters and the analysis has been done for thermal control, but no details or integration have yet been done. It would be very helpful to put together an instrument mockup in order to start sorting out the questions of the basic interior arrangement and mounting points of the instrument. For CRAF, this means probably a 4 sensor package with 4 analog boards, 4 counters, and two computers and power supplies. All this will fit in a package a little smaller than a shoebox. For the contamination control work, probably a much smaller package with just one or two sensors and analog boards would go outside the craft, with the counting and computing probably done by adding a card or two to an existing computer rack inside.

Although the use of the specially developed glass has dramatically reduced the temperature sensitivity of the sensors, the demand for ever higher resolution means that the biggest possible source of error is still temperature control. The sensors have an optimum operating temperature of 32.5 deg C. More important than the actual temperature, however, is keeping a constant temperature over the measurement interval. For particle counting, the measurement interval can be from seconds for large particles up to a few minutes if long averaging times are needed to resolve very small particles. It is relatively easy to keep temperature constant for these short intervals.

The more difficult task is when the item of interest is accumulation over a period of a day or longer. For the CRAF project where power is at a real premium and the temperature control schemes mentioned so far have been mostly passive, it cannot be emphasized too much that holding a constant temperature is much more important and rewarding than staying near any particular temperature. It would be much easier to interpret accumulation data and probably more accurate if the temperature were held at 20 deg C +/- .01, for instance, than if it were held nearer 32.5 but had 1 or two degree swings over periods of a day or two.

For contamination work on the space station, active temperature control to hold +/- .01 deg C is probably no problem. However, one place where tradeoffs have to be made is the expressed desire to hold the stage at different temperatures. It might be possible to hold the sensor body and tapered element at the optimum temperature of 32.5 deg C and the stage at a different temperature, but this has not yet been tried. It might even be possible, although not easy or inexpensive, to customize the glass composition to make the optimum temperature higher or lower.

### 6.3 Integration of Flight Ready Sensors into Flight Instrument

Most all the tasks necessary to take these developed sensors and build an instrument are very straightforward and use commonly available parts and technology. The computer and counter electronics are no different than many digital electronics packages already in space. Even the shutter mechanism and basic structure of the instrument case and view limiters have many similar cousins already in use. Thermal control, however, is going to be the key issue. It will either enhance or degrade the operation of these sensors in direct proportion to the success of the effort put in by the instrument packager and spacecraft thermal control group to understand and use the sensors in the most favorable thermal environment.

APPENDIX I

**RUPPRECHT & PATASHNICK Co., INC.**

*Billing Address:*

P.O. Box 330  
VOORHEESVILLE, N.Y. 12186

*Shipping Address:*

8 CORPORATE CIRCLE  
ALBANY, N.Y. 12203

CONTRACT NAS7-962, SBIR Phase II

A TEOM® Particulate Monitor for Comet and Planetary Atmospheres

Special Report: Vibration Testing of 8 TEOM® Sensor Head  
Assemblies at Acton Labs, February 8, 1988

Prepared by: David Hassel

Conclusion: All 8 TEOM® sensor head assemblies (2 low, 3 med, and 3 high sensitivity) tested survived testing per sec 3.2.2.1 and sec 3.2.3.2 (zone 3) of MMII-3-240 (CRAF AO, Vol. IX: Spacecraft Environmental Design Requirements, July, 1985).

Observations: During the required testing, the TEOM® sensor stages showed no visible movement relative to the heads, i.e. no resonances were excited in the tapered elements. To the extent that the tests represent launch conditions, launch puts less stress on the tapered element than normal operation, in which stage movement is easily discernable.

Discussion:

Tests selected: Section 3.2 of MMII-3-240 includes 7 tests involving shock and vibration: 3.2.2.1, 3.2.2.2, 3.2.3.1, 3.2.3.2, 3.2.4, 3.2.5, 3.2.6. Section 3.2.2.1: Transient events, Spacecraft, is a sine-sweep type test and was selected as one of the applicable tests. Section 3.2.2.2: Transient events, Spacecraft assemblies, was initially selected. At Acton, however, the testing personnel could not agree on a non-ambiguous interpretation of the testing protocol. Inquiries were made to Dennis Kern of JPL, who had signed off that section of MMII-3-240, and his explanation was that indeed the protocol was not clear. He added that the intent of the requirement was to provide a more gentle test for equipment which did not pass 3.2.2.1. After being made aware of the test results from 3.2.2.1 and a further sweep test of 100-400 hz @ 10 g peak, it was his opinion that the test of 3.2.2.2 was superfluous, and need not be run. Section 3.2.3.1 Random Vibration, Spacecraft, is a mild version of 3.2.3.2, Random Vibration, Assemblies. Of these two, 3.2.3.2 was selected, using levels for zone 3, the scan platforms. Section 3.2.4 Acoustic, was reserved for such time as an instrument enclosure is available. Since the instrument will be totally

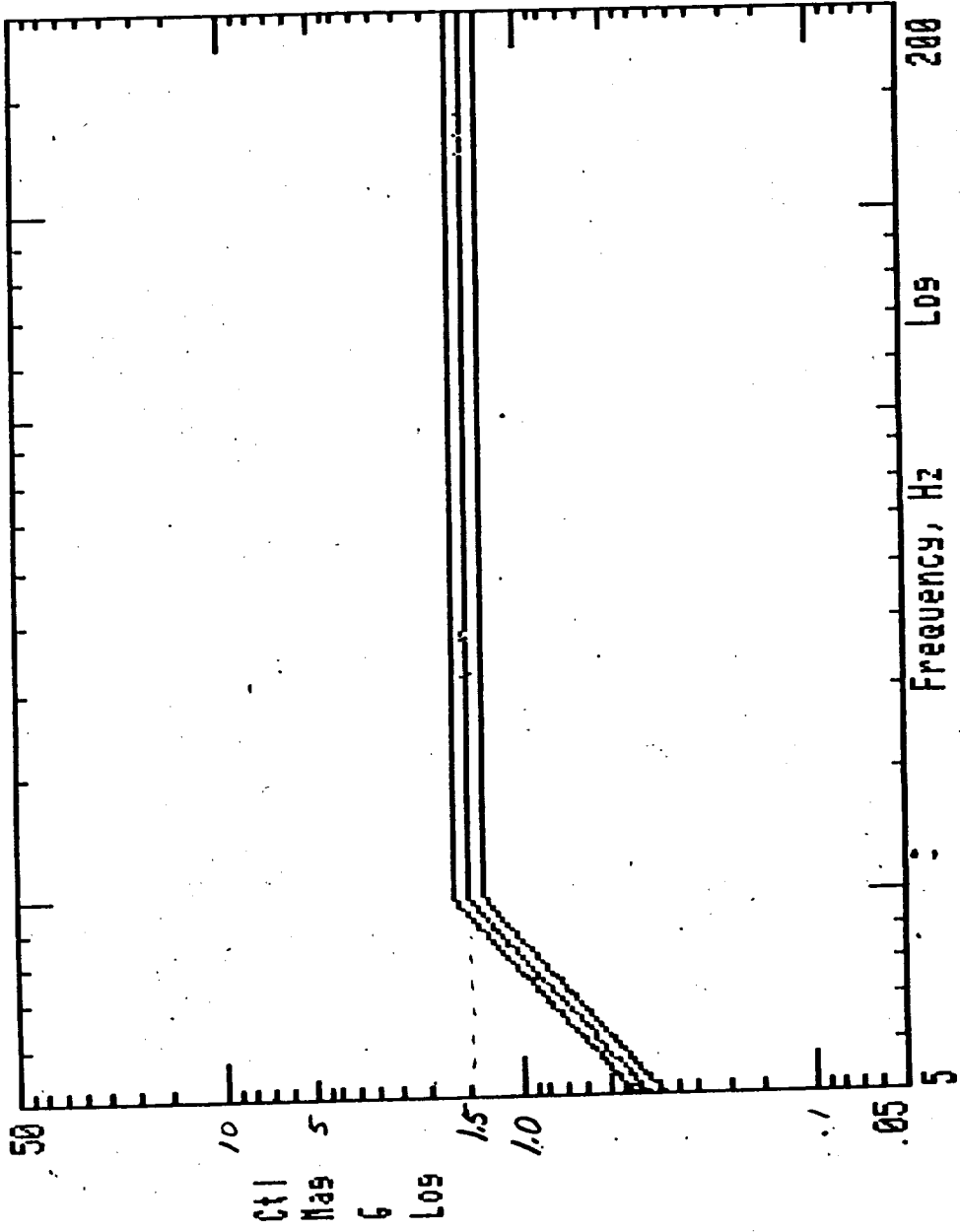
closed during launch (and in any case shuttle launch is not likely), this test was not deemed appropriate at this stage of instrument development. Section 3.2.5: Quasi-Steady Flight Events, involve steady accelerations due to thrust and spin. The maximum g level specified in any direction is 4.5 g. The worst effect on a tapered element would be the apparent 4.5 X increase in mass of the stage. This can be tested by loading the stage while holding the TEOM® sensor head so that gravity pulls the stage in the direction of motion. This amounts to loading of .3 mg on a high sensitivity balance, 3 mg on a medium, and 17 mg on a low. Tests using 1 mg on a high, 5 mg on a medium and 20 mg on a low have been made successfully. Standard laboratory balance calibration weights were used. The weights were affixed by grease, and the only severe part of the test was removing the test weights afterward. Section 3.2.6: Pyrotechnic Shock, was, like the acoustic test, thought more appropriate to run on the complete instrument, rather than on individual sensors.

The sine sweep, random and transient tests were selected and described, and the proposal to run only those three tests was distributed to all interested parties at the Houston meeting. No comments resulted, so it was assumed that everyone was happy with the selected tests.

Description of tests run at Acton: Nine heads were mounted on a 6x6x1 inch aluminum block as specified by Acton. One of each size was a perfect example of the flight design. The others had minor deviations, such as low frequency or high  $m_0$ , but all had proper stage attachment. The block was attached to a cube on Acton's shaker, and moved to various faces of the cube to test the three axes. The programmable shaker produced a real-time plot of the vibration level as the test proceeded. The plots did not differ from axis to axis, so only one example of each is included here. Test 4 is a sine sweep test, 3.2.2.1. Test 6 is a random vibration test, 3.2.3.2. Test 7 is an "extra" sweep test, 10 g peak from 100 to 400 hz (explained in next section). The tapered elements were run before and after the test, but not during.

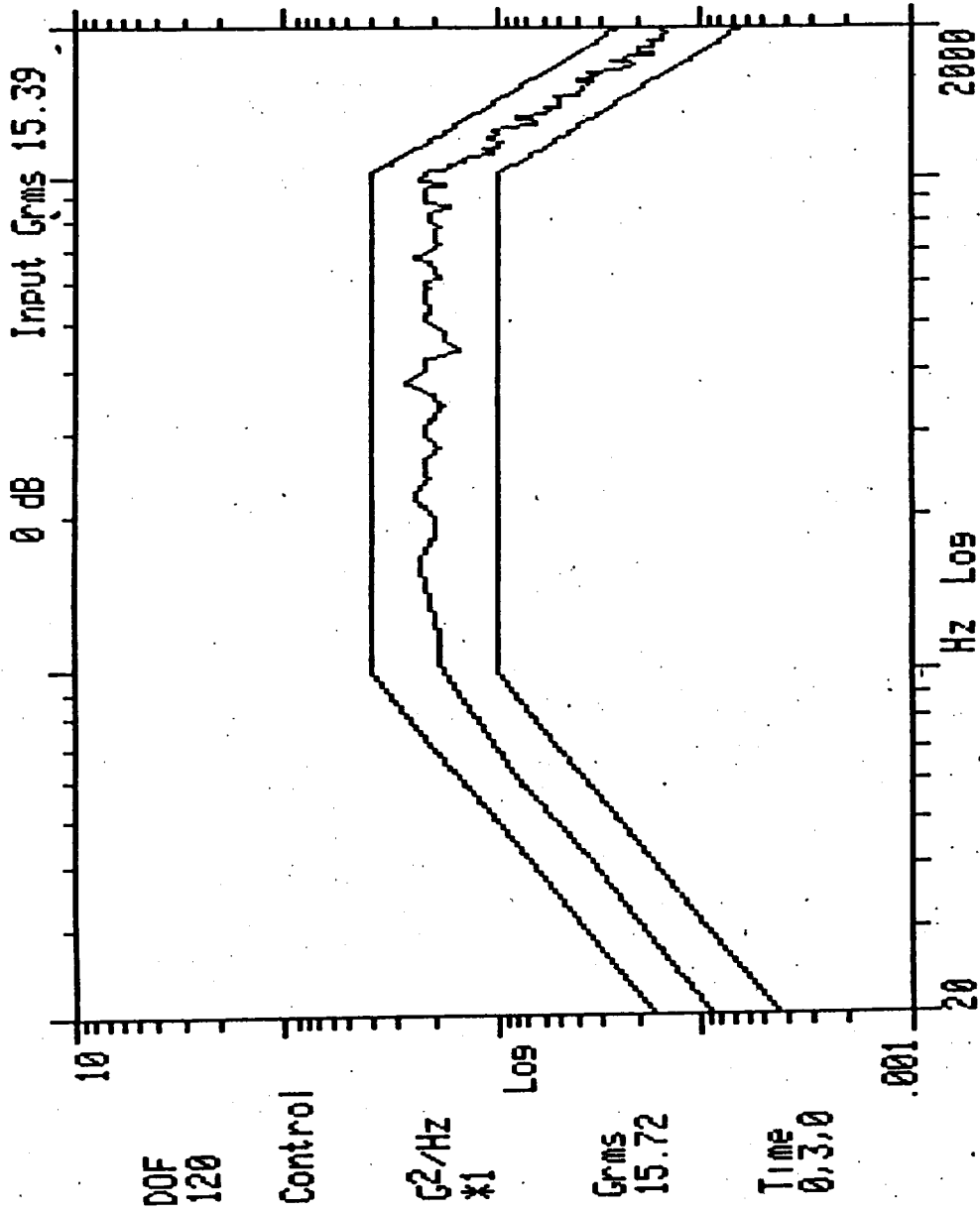
Extra tests and analysis: Certain tests and analyses above and beyond the required ones were also done. An eccentric weight platform was constructed, suspended on low rate springs, and driven using a high speed hand held grinder mounted rigidly on the plate. An accelerometer was also mounted on the plate, and various "g" levels were produced by varying the speed of the grinder and the eccentricity of weights held in its chuck. The accelerometer was monitored on a spectrum analyser, set to plot "g" rms vs frequency. Seven different weights were needed to cover the 5 to 200 hz frequency range, and the output was rich in high frequency overtones, especially over 50 hz. The amplitude of these overtones was often much higher than the primary-rotational frequency amplitude, so at times this test appeared to

Test Completed -- See Post Test Freq 5.000 Sweep 2



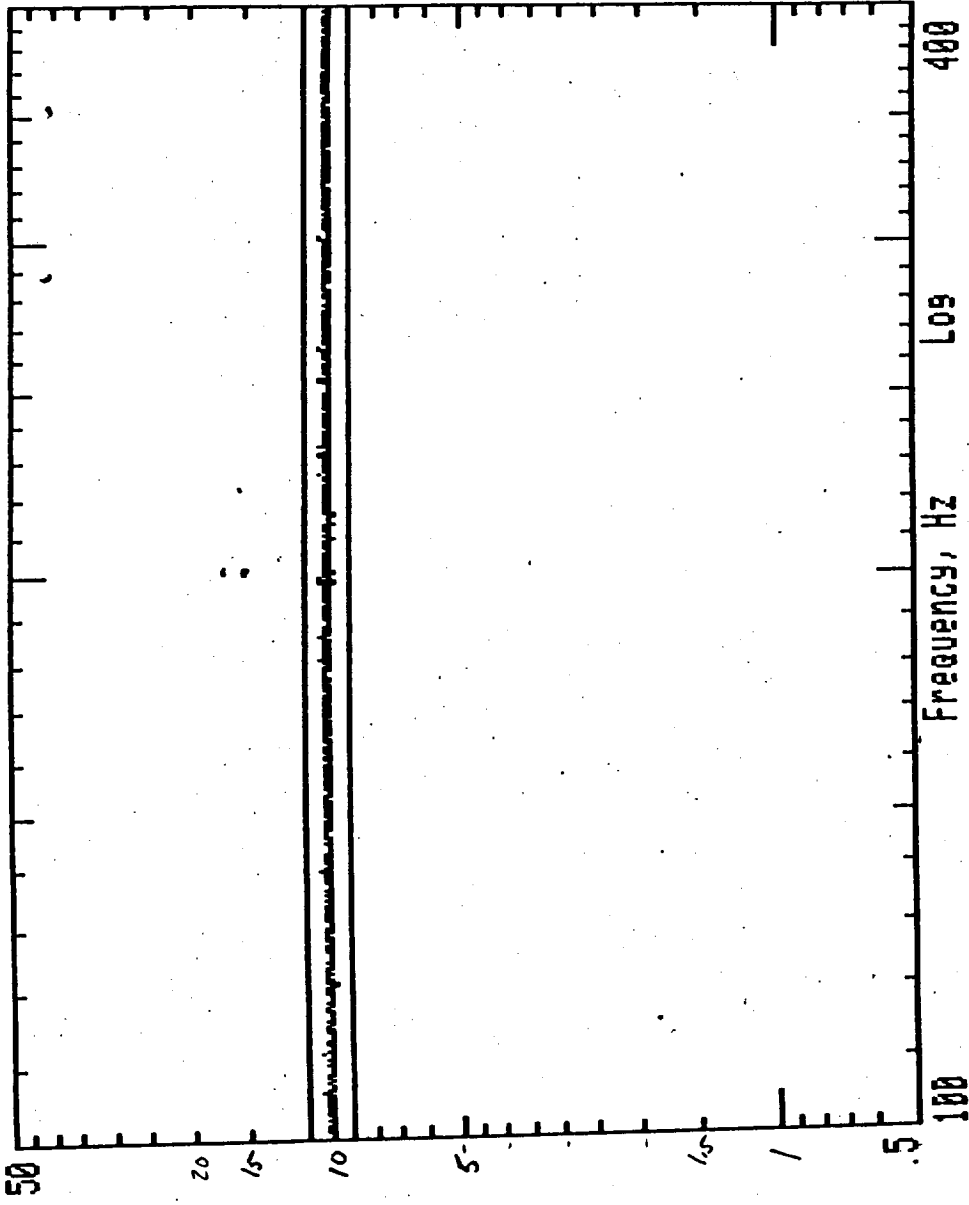
8-Feb-88 TEST# 4 AXIS- X  
14:26:44 24500 R & P SENSOR

Test Completed -- See Post Test



8-Feb-88 A24500 TEST# 6  
14:43:10 R & P SENSOR AXIS- 5

Test Completed -- See Post Test Free 100.0 Sweep 2



Ctl  
Mag  
6  
LOG

8-Feb-88 TEST# 7 AXIS-X  
15:41:32 24500 R & P SENSOR

be testing the tapered elements quite severely. Primary frequency accelerations as high as 3 g rms (4.2 g peak) were run, and swept very slowly compared to the required test rate of 2 oct/min so that resonant amplitudes could build up. At times this caused the tapered elements to oscillate at amplitudes which caused the element to hit the drive plates, but no breakage or damage appeared in any test of any sensitivity element. At least two examples of each size were pre-tested in this severe manner before being taken to Acton.

An analysis program was obtained which allows calculation and plotting of the input and output spectra of a random vibration driven single degree of freedom system (from MTI, Inc. via MACHINE DESIGN, Oct. 8, 1987, with adaptations by R&P). When the random vibration spectrum specified in 3.2.3.2 was input to this program, along with damping factors for the various tapered elements, the rms displacement predicted for the stages was .075 inch p-p in vacuum for the tapered element with the highest Q. This is an entirely acceptable amplitude. In air, or with lower Q, the amplitude would be less. The prediction for the low sensitivity element in air was .045 in p-p, or about 1 mm. In the testing at Acton, it did not appear that the stage moved even this amount relative to the housing, even though 1/2 mm p-p would probably have been visible. The rms value, of course, is a statistical value, and occasional excursions of this size could have been missed. There was certainly no "driving" of the tapered element by the random vibrations in such a way as to produce any steady amplitude.

Since the tapered element operating frequencies are being targeted between 200 and 250 hz, and the cross direction frequencies between 300 and 375 hz, it was deemed interesting to investigate the tapered elements' response to a sweep which covered this range. Accordingly, a test was specified which resembled test 3.2.2.1 (1.5 g peak swept from 5 to 200 hz @ 2 oct/min). The test chosen was 10 g peak swept from 100 to 400 hz @ 2 oct/min. A slight trembling of one medium tapered element with a 1.5 X overweight stage was noticed. The other 7 tapered elements showed no movement relative to the housings. For a steady input at the resonant frequency, one would expect the tapered element amplitude to go to Q times the input amplitude, but the Q of these elements is so high, even in air, that only a few cycles of any given sweep are at a frequency which could put significant energy into the tapered element. No amplitude can build up. The high Q of these elements, as has been stated many times before, is what protects them. They will only accept energy when it is precisely at their resonant frequency, and only when it lasts long enough (and in coherent phase) to build up the amplitude over many cycles. Such a disturbance is hard to even imagine, and the amplitude of random noise needed to raise the probability that it contained such a component would wreck the rest of the spacecraft long before the tapered element was affected.

## APPENDIX II

### Specifications of All Sensors Cited

No.	Nominal size cm <sup>2</sup>	m <sub>o</sub> w/o stage	m <sub>o</sub> w/ stage	K <sub>o</sub>	Freq.	Notes
501	.01	1.4 x 10 <sup>-5</sup>		1.6	338	No stage
*507	1	7 x 10 <sup>-4</sup>	4 x 10 <sup>-3</sup>	248	247	Hand made TE
602	.1	1.4 x 10 <sup>-4</sup>		29.4	448	No stage
606	.01	4.6 x 10 <sup>-5</sup>	7.6 x 10 <sup>-5</sup>	327	328	Heavy
*923	.1	7 x 10 <sup>-5</sup>	4 x 10 <sup>-4</sup>	18	210	Small blemish gold coat
*924	.01	4 x 10 <sup>-5</sup>	7 x 10 <sup>-5</sup>	3.86	224	Low ellipticity
*926	.1	8 x 10 <sup>-5</sup>	7 x 10 <sup>-4</sup>	19	153	Alpha stage, heavy
*927	1	2.5 x 10 <sup>-4</sup>	3 x 10 <sup>-3</sup>	161	214	Final form of 1 cm <sup>2</sup>
*930	.01	3 x 10 <sup>-5</sup>	5.8 x 10 <sup>-5</sup>	2.63	212	Final form of .01 cm <sup>2</sup>
*932	.01	3.6 x 10 <sup>-5</sup>	6.5 x 10 <sup>-5</sup>	2.93	290	Small defect in stage fusing
*934	.1	9 x 10 <sup>-5</sup>	3.7 x 10 <sup>-4</sup>	22.1	244	Final form of .1 cm <sup>2</sup>

500 series: hand made LC glass, lab batch  
 600 series: hand made, LC glass, production batch  
 900 series: machine made, LC glass

\* Vibration tested